Journal of Electrical Engineering and Modern Technology

Volume No. 13

Issue No. 2

May - August 2025

ENRICHED PUBLICATIONS PVT. LTD

S-9, IInd FLOOR, MLU POCKET,
MANISH ABHINAV PLAZA-II, ABOVE FEDERAL BANK,
PLOT NO-5, SECTOR-5, DWARKA, NEW DELHI, INDIA-110075,
PHONE: - + (91)-(11)-47026006

Journal of Electrical Engineering and Modern Technology

Aims and Scope

Journal of Electrical engineering and Modern Technology, publishes original research papers in the fields of Electrical and Electronic Engineering and in related disciplines. Areas included (but not limited to) are electronics and communications engineering, electric energy, automation, control and instrumentation, computer and information technology, and the electrical engineering aspects of building services and aerospace engineering, Journal publishes research articles and reviews within the whole field of electrical and electronic engineering, new teaching methods, curriculum design, assessment, validation and the impact of new technologies and it will continue to provide information on the latest trends and developments in this ever-expanding subject.

Journal of Electrical Engineering and Modern Technology

Journal of Electrical Engineering and Modern Technology

(Volume No. 13, Issue No. 2, May - August 2025)

Contents

Sr. No.	Article / Authors Name	Pg. No.
1	Real Time Visitor Identification Management System - *Waseem Tamboli*	1 - 6
2	PLC based Waste Management Robot - *Siddharam, D S Suresh, Rajendra C J, Sekar R*	7 - 12
3	Power Quality Improvement in an Inverter Controlled Three Phase Distributed Generation System - *B Rajendra Prasad Tenali, V. S. Vakula*	13 - 24
4	High Performance Portable Charger - *Sangita Mishra, Manoj Kumar Swain*	25 - 32
5	LLC Resonant Inverterfor Solar PV Applications - *Kirlampalli Harija Rani, C H Venkateswara Rao*	33 - 41

Real Time Visitor Identification Management System

Waseem Tamboli
Electronics & Telecommunication engineering , Department of E&TC, NBN Sinhgad School of Engineering, Pune, India, E-mail: waseemstamboli@gmail.com

ABSTRACT

Face recognition is one of the most trustworthy form of biometric as compared to other form of biometrics. The paper presents a Home security based system using face recognition and alerting the owner of the house by providing messaging alerts on cell phone. The application runs in real time environment by identifying the persons from captured image. Localization and Recognition are the two important scenarios on which the performance of the systems depends undoubtedly. Once the system localizes the faces from the captured image, recognition part is processed further. After successful recognition of the person, the door will be opened automatically. Various issues regarding successful localization of faces have also been put forth in this paper. Satisfactory results in correct localization and recognition of persons are obtained by experiments.

Keywords—Face Detection, Face Recognition, Biometric, Home Security, Message Alerts.

I. INTRODUCTION

Many methods are available in biometric identifications such as fingerprint, eye iris, retina, voice, face etc. These different methods have certain advantages and disadvantages which must be taken into consideration while developing biometric systems, such as system reliability, price, flexibility, necessity of physical contact with the scanning device and many other parameters. Hence considering above parameters face is such a biometric which does not require any physical contact with scanning device. Also fraud cases are negligible as compared to other biometrics exception in case of identical twins. Accuracy of face recognition system varies as per the images captured in controlled environment against that of un- controlled environment. Illumination and clear background are the primary concern for building a successful face recognition system [1]. Unless and until a well addressed image is been captured, the processing of image cannot be processed further. A very efficient technique called image retargeting is proposed by Wenyu Hu et al. [2] in which it helps to identify the area of interest from an image whereas the unwanted areas of the image are sacrificed. Image retargeting technique can be useful in case of face detection systems by identifying only the faces from the image and neglecting the unwanted area. Real time image capture also possess problem such as facial pose, lighting and poor image resolution [3]. Hence above parameters are to be taken into consideration while building the system. Many other experts who have proposed their work related to face recognition system suggest that the image to be captured must not contain noisy data [4], which may lead to poor image quality resulting into failure of the system. The problem of visual face recognition affecting by pose variation, expressions, light intensity are overcome by 3D technology [5] where 3-D face recognition can achieve higher recognition accuracy than visual face recognition system. A concept of perfect recognition and

its analysis is put forth by Wang et al. [6] to model the system performance without training data. This method helps to improve the performance of recognition system. Srinivasan et al. [7] explored the use of region covariance matrices for face recognition as a set of holistic face image feature. But the main drawback lies with the description which does not lie in Euclidean space. Prototype modeling proposed by Dahmane et al. [8] successfully identified the facial expressions with a recognition rate of 86.69% for better recognition technique. A simple and flexible system for face image quality assessment, in which multiple feature fusion and learning to rank are proposed by Jiansheng Chen et al. [9].

II. SYSTEM ARCHITECTURE

2.1. Proposed System

The main objective of the proposed system is to provide a better security for home applications where both husband and wife are working, leaving their elderly parents and small kids alone at home. As the system is completely automatic it involves zero man power. Image captured through an appropriate camera will undergo various processing steps as described in the design flow later on. If an authenticated person is recognized, the door will be opened automatically. But if an unknown person or an intruder is detected, an alerting message will be delivered to the owners cell phone as well as a buzzer will blow alerting the persons that are present within the house. No any advanced components are required for building up the proposed system. Existing webcams, security cameras are sufficient for capturing the images. Apart from the camera, selection of each hardware resource is made as per the design requirement of the system. Even the GSM module has been replaced by one of the SMS sending services which has reduced the cost of the system considerably. The most important part of the systemrelies on localizing the faces from the captured image. Once the localization module is successful, recognition module proceeds as per the defined algorithms in the design flow shown below.

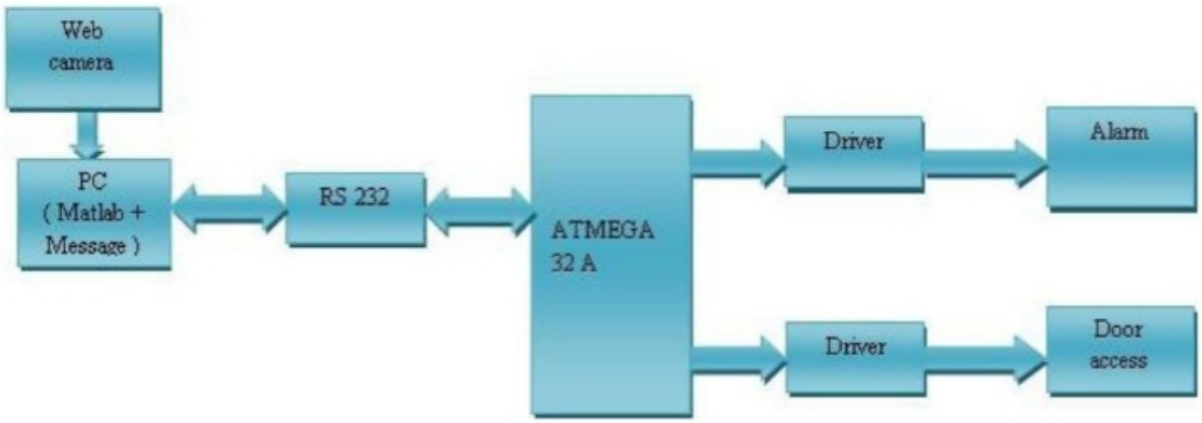

Fig. 1. Block diagram of Proposed System

Here we present an automatic face recognition system for the application of door access control system. The proposed systems reliability depends upon three subsequent phases that are-face

detection, face recognition and automatic door control action. In this paper we represent, an automated face recognition system, whose application is designed for the purpose of door access control system. Fig. 1 represents the block diagram of the proposed system architecture along with its setup and connections.

III. DESIGN FLOW

Fig 2. shows the overall design flow, related to face local- ization, feature extraction and face recognition of the individ- uals. The proposed face recognition system involves various algorithms such as blurring, RGB to HSV, thresholding, blob detection, cropping, gray scaling, edge detection and extraction process.

Blurring: It helps to reduce image noise and reduce details by eliminating high frequency components from an image acting as a low pass filter.

RGB to HSV: RGB color space describes colors in terms of amount of red, green and blue present. HSV describes colors in terms of hue, saturation and value. Also it describes color using more familiar comparisons such as vibrancy, color and brightness. Skin color thresholding: Thresholding helps to convert obtained image in terms of black and white. A specific threshold value is set. If the value of required pixel is above threshold value, it is labeled as 1 and if it is less, it is labeled as 0.

Blob detection: It helps to identify the region of interest.

Once the region of interest is identified, further processing becomes simpler.

Face localization: In proposed system, the region of interest will be the face. Further, once the face gets localized, the unwanted part of the image is excluded and face gets cropped. Gray scaling: Every gray scaled image contains information in terms of range between black and white color. Every pixel carries a gray scaled value.

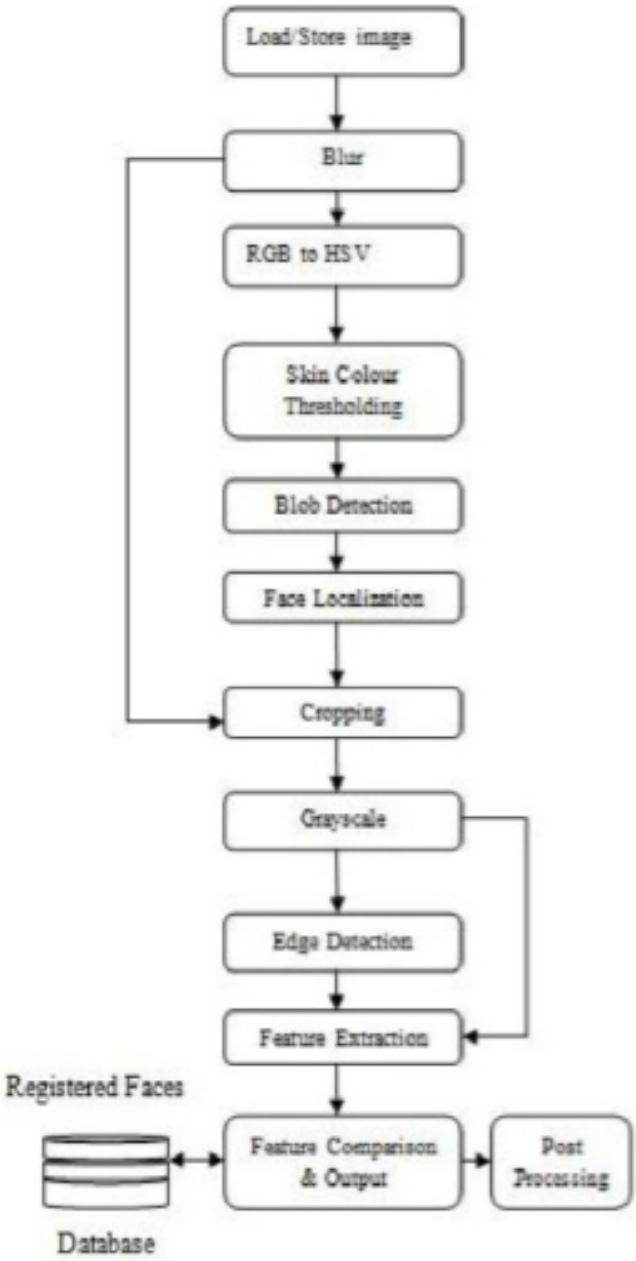

Fig. 2. Design Flow for Face Recognition

Edge detection: It significantly reduces the amount of data and filters out useless information while preserving important structural properties in an image.

Feature Extraction: Once the above algorithms are pro- cessed, relevant features from the image are extracted and compared with that of initially stored image performing further door accessing action.

IV. EXPERIMENTAL RESULTS

As discussed below, the experimental results depicted are, the system successfully identifies the face from captured image and indicates whether it is authenticated or not as shown in fig 3. If authenticated

person is recognized, door gets opened as shown in fig 5. If an unauthenticated person is recognized, refer fig 4. the door remains closed as in fig 6. An alert message will be delivered to the owners cell phone as indicated in fig 7. Also a buzzer will be sound to alert the house users that are present within the house. Whereas in case of an authenticated person, the door gets automatically opened and provides access to the user.

Fig. 3. Authentication successful for Registered User.

Fig. 4. Authentication failed for Unknown User.

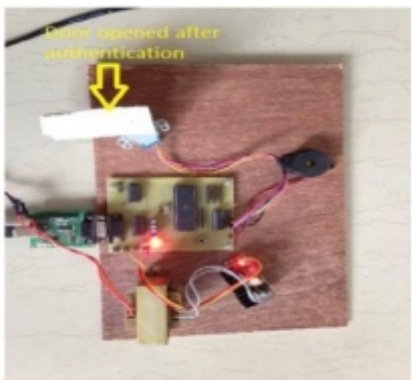

Fig. 5.Door opened after successful Authentication.

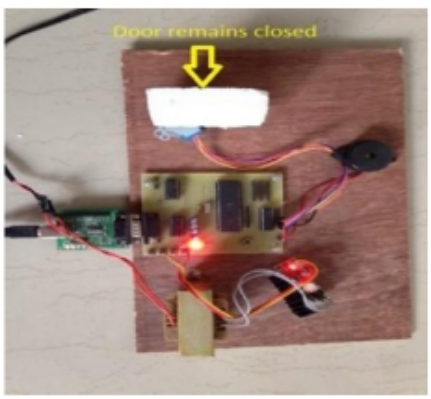

Fig. 6. Door remains closed for Unauthorized Authentication.

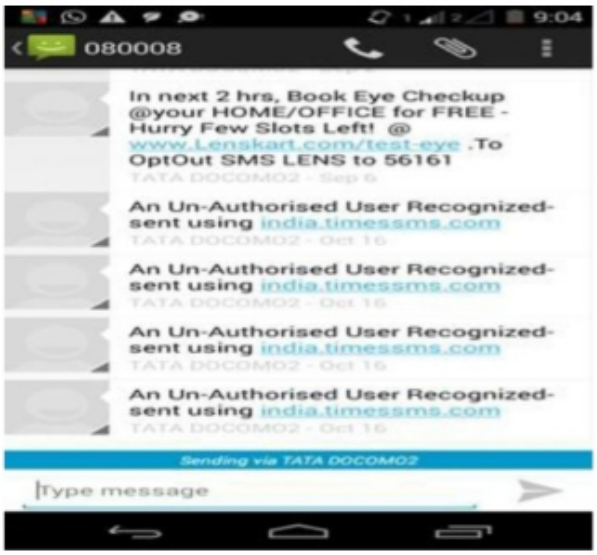

Fig. 7. Alert message on Owner's Cell Phone.

CONCLUSION

In this paper, we have developed such a face recognition system which is reliable under controlled environment. As compared to other existing biometric techniques, face recogni tion can be considered as the most effective mean of security system due to its various advantages. Various algorithms defined in the design flow, when integrated in the system, help to build up the overall system of face recognition which is very secure. The system is very cost effective as no any expensive device is been used. Alert messages are successfully delivered to the owners cell phone through SMS messaging services. The system can be made robust by improving the detection and recognition of faces under uncontrolled environments.

REFERENCES

[1] Wonjun Hwang, Haitao Wang, Hyunwoo Kim, Seok- Cheol Kee, and Junmo Kim, "Face Recognition System Using Multiple Face Model of Hybrid Fourier Feature Under Uncontrolled Illumination Variation" IEEE Transactions on Image processing, Vol. 20, No. 4, April 2011.

[2] Wenyu Hu, Zhongxuan Luo, and Xin Fan, "Performance Modeling and Prediction of Face Recognition Systems."IEEE Journal on emerging and selected topics in circuits and systems, Vol 4., No. 1, March 2014.

[3] Peng Wang and Qianj Ji, "Image Sensor-based Heart Rate Evaluation from Face Reflectance Using Hilbert-Huang Transform." IEEE proceed- ing for computer society conference on computer vision and pattern recognition, 2006.

[4] Unsang Park, Anil K. Jain and Arun Ross, "Face recognition in video: Adaptive Fusion of Multiple Matchers." IEEE Transactions, 2007.

[5] Sumit Shekhar, Vishal M. Patel, Nasser M. Nasrabadi, and Rama Chel- lappa, "Joint Sparse Representation for Robust Multimodal Biometrics Recognition." IEEE Transactions on Pattern Analysis and Machine Intel- ligence, Vol 36, No. 1, January 2014.

[6] Hailing Zhou, Ajmal Mian, Lei Wei, Doug Creighton, Mo Hossny, and Saeid Nahavandi ,"Recent Advances on Singlemodal and Multimodal Face Recognition: A Survey" IEEE Transactions on Human Machine Systems, 2014.

[7] Ramya Srinivasan, Abhishek Nagar, Anshuman Tewari, Donato Mitrani, and Amit Roy-Chowdhury , "Face Recognition Based On Sigma Sets Of Image Features" IEEE Transaction on International Conference on Accoustic, Speech and Signal Processing, 2014.

[8] Mohamed Dahmane and Jean Meunier "Prototype-Based Modeling for Facial Expression Analysis. IEEE Transactions on Multimedia, Vol. 16, No. 6, October 2014.

[9] Jiansheng Chen, Yu Deng, Gaocheng Bai, and Guangda Su , "Face Image Quality Assessment Based on Learning to Rank." IEEE Signal Processing Letters, Vol. 22, No. 1, January 2015.

PLC based Waste Management Robot

[1] Siddharam, [2]D S Suresh, [3]Rajendra C J, [4]Sekar R
[1,2,3,4]Dept. of ECE, CIT, Gubbi, Karnataka, India
E-mail: [1]sidd.i4575@gmail.com, [2]sureshtumkur@yahoo.co.in, [3]rajendracj@yahoo.com,
[4]sekar.rp@gmail.com

ABSTRACT

Usually food waste which comes out of the kitchen is simply dumped into the dumping yard. The food waste and rotten things will end up in land fill and further it turns into methane. Methane is considered as green house gas that is particularly damaging to the environment and also causes severe health diseases among public. To overcome this problem a product has been developed using Programmable Logic Controller (PLC) which converts waste into fertilizers. In this system, the grinded kitchen waste pass to the heating chamber to convert the gel form of material into a dry product. The dry form of product can be used as manure. Proposed system consumes less time for completing the process and its performance has been verified by implementing hardware. Since, the hardware components used in this system is less so that it's a cost effective system.

I. INTRODUCTION

In mechanical based industries waste recycling process is carried out by using programmable logic controller. Using this mechanism metals are separated from waste material. A programmable logic controller based prototype is developed for separating out metals from waste material. In this system metal sensors are used to detect metals from waste material. The detected metals are deposited into a bin and waste material dumped into a waste bin.

In metropolitan cities factories are intended to manufacture some useful product from waste material coming from different places. This project mainly concentrates on the waste coming out of kitchen. Available mechanism takes lot of time and high cost to convert the kitchen waste into fertilizers because collection of waste material takes lot of time to convert that waste material into fertilizers which is required for plants growth. In this project a PLC based system is developed which is used to process the waste into a dry form of product. This system overcomes the disadvantages like high cost and more time.

Connected Components Workbench (CCW) is a software tool used in this project for drawing the ladder diagram. This software tool is selected because it has both offline and online capability and it also support the free software update.

II. PROBLEM STATEMENT

Fertilizers are essential nutrient for the growth of the plants and trees. The available industries take lot of time to manufacture the fertilizers because it takes lot of time to collect the waste and also has high cost to manufacture the fertilizers.

III. METHODOLOGY

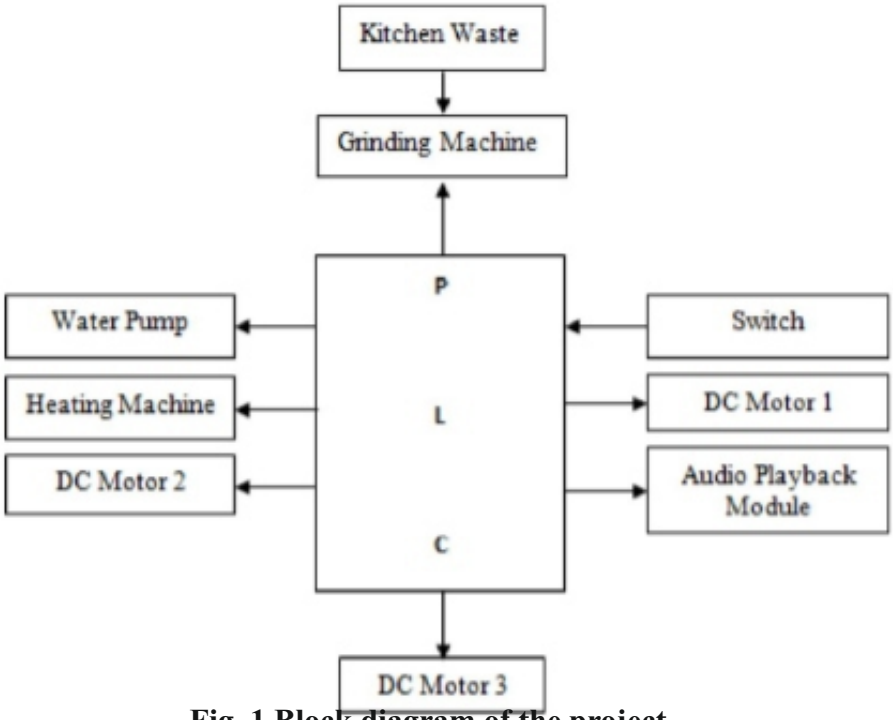

Fig. 1 Block diagram of the project

In figure 1 the kitchen waste taken into the grinding machine then the grinding machine start to grind kitchen waste into a gel form of material. The output of the grinding machine given to the heating chamber to convert the gel form of material to the dry form of product which can be used as natural manure.

IV. HARDWARE REQUIREMENTS

4.1 D. C Motors

DC motor convert the electric energy into mechanical energy when the current flows through wires the magnetic field is generated this magnetic field reacts with outside static magnets field. The interaction of these two forces produces the movement of the shaft and motor develops the motion with the help of some magnets.

4.2. Mixer

Mixer operates at 230v AC supply and the main function of the grinding machine is to grind the waste taken in the jar. Mixer converts the solid form of the waste into a liquid or gel form of material by rotating the blades.

4.3 Heating Machine

The heater uses the 230v AC power supply to heat the outcome of grinding machine. Using electric heater evaporate the water content present in the liquid form material. The output of the heater is in the form of solid which can be used as fertilizers in agriculture field.

4.4 Relay

Relays are used to separate two circuits electrically and connect them magnetically. Double Pole Double Through (DPDT) relays are used to power wither device/appliance or another and also used to change the polarity at the terminals of the device at the output terminals.

When voltage is applied to the relay circuit the current flows which results the magnetic field with the help of magnetic field the contact point to the relay comes into motion.

In this project relays are used for opening and closing the bottom valve i.e, valve 2 and also the front and back movement of the container which is placed on the heater.

4.5 Power supply

There are two power supplies are required one for DC motor rotation and one for PLC. Power supply contains a step-down transformer. The primary coil operates at 230v and secondary at 12v and 1A current. The output of the transformer given to the bridge wave rectifier. The main function of the bridge wave rectifier is to convert alternating voltage (A.C) to pulsating direct voltage (D.C). Bridge wave rectifier operates in two modes i.e., positive half cycle of A.C signal and negative half cycle of the A.C signal. Bridge wave rectifier contains four diodes.

4.6 Audio playback module

Audio playback module consist of so many components i.e., it consist of some LED's, capacitors, resistors etc. so all these components are connected on a single board. The VS 1000 module can be used as audio playback module and it reduces the man effort by initially recording the man voice.

4.7 Programmable Logic Controller (PLC)

This project uses micro830 programmable logic controller and it operates at 24V DC voltage and PLC micro830 has 14 input pins and 10 output pins.

In industries machine designers require a less cost controller for their small applications and this requirement is satisfied by the Allen-Bradley micro800 programmable logic controllers and a software called connected component workbench.

V. SOFTWARE REQUIREMENT

Connected Components Workbench design and configuration software provides controller programming, device configuration and also HMI editor. So some technologies like proven Rockwell Automation and Microsoft Visual Studio technology, Connected Components Workbench software help us to minimize initial machine development and also minimises initial time to set-up controls with the help of free software download IEC 61131-3 standard.

This freely available standard software updates and also help us to minimise effort. Connected Components Workbench software minimises initial machine development.

VI. RESULTS

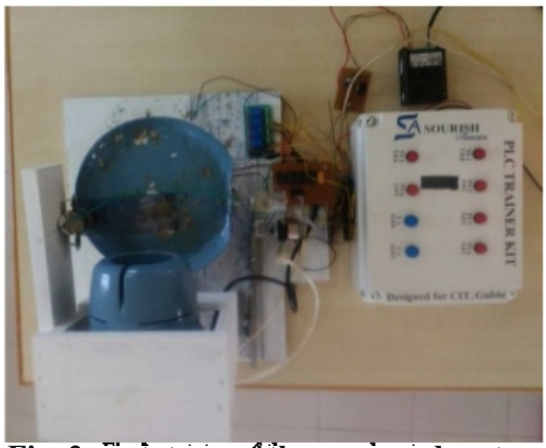

Fig. 2 prototype of the proposed system

The entire operation of the system is described by voice playback module. The entire set up of the proposed model is as shown in figure 2. Using PLC based waste management system convert kitchen waste into natural manure that has been used in agriculture field.

CONCLUSION

Using this PLC based waste management system, convert the waste coming out from the kitchen is converted to a fine dry form of the product. The obtained product can be used as fertilizers (natural manure) and the whole process to prepare natural manure takes less time around 20-30 minutes. because

SCOPE OF THE FUTURE WORK

The proposed system mainly for household kitchen waste management system can be extended for large hotels and restaurants. so that, the large quantity of waste can be reproduced as a manure. The designed system facilitated with audio playback and display. So that, the people who are not able to read or write can know the status of the process.

REFERENCES

[1] "Waste segregation using programmable logic controller" by M .Dudhal, B. S. Jonwal and Prof. H. P. Chaudhari International Journal for Technological Research in Engineering Volume 1, Issue 8, April-2014.

[2] "Automated waste shorter with mobile robot delivery waste system" by Fitzwatler G. Ang , Maria Karla Angel R. Gabriel , Jameson Sy , Jenny Jane O. Tan and Alexander C. Abad IEEE Proceedings of the Image and signal processing, 2010 3rd international congress (pp. 1657-1661).

[3] "Automation and robotics in post disaster waste management" by Gayani Karunasena, Dilanthi Amaratun and Richard Haigh UNEP (2005) Natural Rapid Environmental Assessment – Sri Lanka, UNEP Sri Lanka Country Report – 2005.

[4] "Automated garbage collection robot" by Ruide (Ray) ,Che n Scott Chu, Bao Nguyen and Kevin Tan vol. 6, no. 1, 2009.

[5] "Robotic arm pick and place system" by Mark Anthony B. Mabanta, Jerome P. Pabillaran, and et.al. Engr. Maridee B. Adiong SRI International, Mitsubishi Electric Company, 1988.

[6] "Aroma Encapsulation in Powder by Spray Drying, and Fluid Bed Agglomeration and Coating" by Turchiuli Christellea,b, Cuvelier Marie-Elisabetha, Giampaoli Pierrea, and Dumoulin Elisabetha AgroParisTech, UMR1145 Ingénierie Procédés Aliments, F-91300 Massy, France Univ Paris-Sud, Orsay, F-91405, France 1999.

Power Quality Improvement in an Inverter Controlled Three Phase Distributed Generation System

[1] B Rajendra Prasad Tenali, [2]V. S. Vakula
[1]Research Scholar, Dept. of Electrical and Electronics Engg JNTUK, Kakinada
[2]Asst. Professor, Dept. of Electrical and Electronics Engg JNTUK- University College of Engineering Vizianagaram Campus, Vizianagaram
E-mail: [1]rajendratce@gmail.com, [2]dr.vakulavs.jntu@gmail.com

ABSTRACT

Due to the presence of non-linear loads such as switching mode power supplies and phase controlled rectifiers or alternating current converters for electronic converters used on utility side in a network consisting of 3-phase DG source, a nonsinusoidal voltage is absorbed at the point of common coupling (PCC). The situation gets aggravated during the islanding mode, when the grid power is not available. This deteriorates the performance of other loads connected in parallel. A scheme based on nonsinusoidal pulse-width-modulation (NSPWM) control of an inverter-based 3-phase DG source is implemented to regulate and produce a sinusoidal voltage at the PCC. It is demonstrated that THD of the supply voltage at the PCC can be reduced to the desired level.

Keywords- Distributed generation (DG), Nonsinusoidal Pulse-width Modulation (NSPWM), Point of Common Coupling (PCC)

I. INTRODUCTION

FROM the viewpoint of limited reserves of conventional fuels, distributed generation (DG) systems such as photo voltaic (PV), wind, fuel cells, micro turbines, etc. are expected to increase. With the increased distributed resources (DR) into the grid, it is desirable and advantageous to tap additional benefits out of these resources besides their main function of active power generation. The feasibility of using DG for power conditioning, power factor compensation, real and reactive power control, and mitigation of other power-quality (PQ) problems have been discussed in the literature [2]–[5]. A hybrid DG system based on the PV-cell combination, which is capable of regulating reactive and active power fed into the grid, has also been presented [5].

All of the work cited refers to the grid-connected operation of DG sources. To realize the full potential of DG units, however, their operation under stand- alone mode (i.e., in an islanded mode, must also be investigated [6]). This is because the system performance in stand-alone mode is more sensitive to factors such as the control scheme of the DG, interface, and types of loads etc., compared to grid-connected operation.

Fig. 1 shows the interface of a inverter-based DG unit operating in stand-alone mode. VS represents the rms value of the AC voltage generated by the inverter. The DG source is tied to the point of common coupling (PCC) through an inverter and a series inductor having an inductance “r” and an internal

resistance “L,” The series inductor is essential from the control and protection point of view [7]. If the grid is live, the quality and magnitude of the voltage at the PCC is decided entirely by the grid. As the grid imposes a stiff sinusoidal voltage at the PCC, irrespective of the presence of nonlinear loads, other loads connected at the PCC draw sinusoidal current. Thus, the presence of nonlinear loads does not affect the performance of other loads connected at the PCC as long as the grid is live. However, if the grid is not live and if the DG source has to supply power to the loads connected at the PCC, the presence of nonlinear loads affects the performance of all the loads connected at the PCC. In this case, the nonlinear current, drawn by the nonlinear load, leads to a nonlinear voltage drop across the line impedance, given by

$$V_{line} = V_1 + \sum V_{hn} \qquad (1)$$

where V1 is the fundamental component of V_{line} and V_{hn} represents its nth harmonic component.

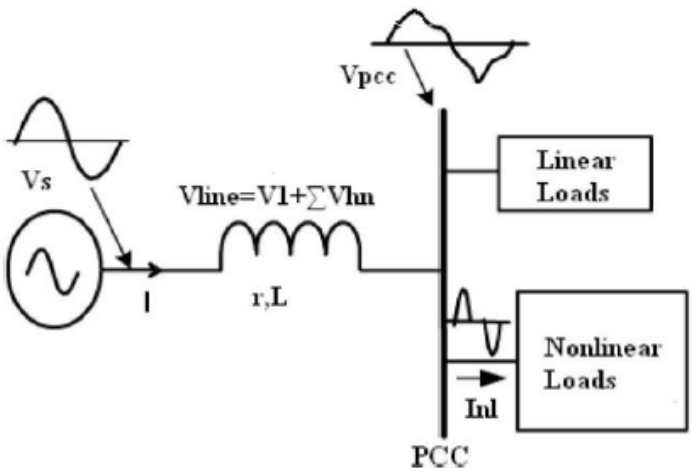

Fig 1: DG source interface with the loads at the PCC.

Hence, even if the inverter is controlled to generate a sinusoidal output voltage, the voltage at the PCC VPCC=VS-V_{line} will be nonsinusoidal. The problem of distorted supply voltage at the PCC, as shown in Fig. 1, can be handled by compensating the nonlinear drop across the line impedance.

The remainder of this paper is organized as follows. Section II explains the principle on which the proposed scheme works. It describes the analytical background of the scheme to regulate the voltage at the PCC and to compensate the harmonic voltage drop across the line impedance. Section III gives the details of the control scheme based on the analysis presented in Section II. Section IV presents the simulation results. The major conclusions of the work are presented in Section V.

II. ANALYTICAL BACKGROUND

This section describes the analytical background of the scheme to regulate the voltage at the PCC and to compensate the harmonic voltage drop across the line impedance.

The principle involved to regulate and achieve a sinusoidal supply voltage at the PCC is mathematically explained in this section. Referring to Fig. 1, the voltage at the PCC is given by

$$V_{PCC} = V_S - I(r + j\omega L) \quad (2)$$

where VPCC, VS, and I represent the vector quantities and consist of fundamental as well as harmonic components. I is the current supplied by the source (inverter).

Hence

$$V_{S1} + \sum_{n=2}^{k} V_{Sn} - I_1(r + j\omega L) - \sum_{n=2}^{k} \{I_n(r + j\omega L)\} = V_{PCC1} + \sum_{n=2}^{k} V_{PCCn} \quad (3)$$

where VS1, VPCC1 and I1 represent the fundamental component of the source voltage, voltage at the PCC, and source current respectively, while VSn, VPCCn, and In are the nth order harmonic components present in the source voltage, voltage at the PCC, and source current, respectively. k is the maximum order of harmonics which has to be eliminated.

Rearranging (3) yields the following:

$$\{V_{S1} - I_1(r + j\omega L)\} + \sum_{n=2}^{k} \{V_{Sn} - I_n(r + j\omega L)\} = V_{PCC} = V_{PCC1} + \sum_{n=2}^{k} V_{PCCn} \quad (4)$$

Hence, if the second term on the left-hand side of (4) is made zero, a sinusoidal voltage at PCC can be obtained. Thus, (4) shows that in order to achieve a sinusoidal, the following condition should be satisfied:

$$\sum_{n=2}^{k} \Delta V_n = \sum_{n=2}^{k} V_{PCCn} = 0 \quad (5)$$

where

$$\Delta V_n = V_{Sn} - I_n(r + jn\omega L) \quad (6)$$

Thus, to achieve a sinusoidal voltage at the PCC, each "n" harmonic component (V_{PCCn}), in V_{PCC} must be made zero. It is evident from equations (5) and (6) that this will lead to $\Delta V_n = 0$, thereby compensating the nonlinear drop across the line impedance on the source side. This can be done by comparing each harmonic component V_{PCCn} with the desired (tolerable) level V_{PCCn*}, resulting in the error voltage as given below

$$x_n = |V_{PCCn}*| - |V_{PCCn}| \quad (7)$$

where xn, given by (8), is then applied to the individual proportional-integral (PI) controller whose output is multiplied with a sine wave at the respective harmonic frequency and delayed by an angle θn identical to that of the phase of that harmonic in the output voltage. This results in the corresponding "reference harmonic component", V_{PCCn}..

Thus

$$V_{PCCn}^{*} = \{k_p x_n + k_i \int x_n dt\} \times k_n \sin(n\omega t + \theta_n) \quad (8)$$

where kp and ki are the proportional and integral constants. While kn is the amplitude of the nth harmonic component with which the reference sinusoid waveform of SWPM is to be modulated. Here, modulation refers to the addition of the "reference harmonic components" to the reference sinusoid waveform of SPWM for inserting the nonlinear voltage ΣVhn in series with VS (Fig. 1).

The above reference harmonic components shown in equations (7) and (8) modulate the sinusoidal reference V1* in such a way that a particular harmonic component is produced in the output of the inverter which opposes its counterpart on the load side. The resulting reference waveform is a nonsinusoidal reference waveform Vref*, which is used for comparison with a carrier triangular waveform. Therefore

$$V_{ref}^{*} = \sum_{n=2}^{k} V_{PCCn}^{*} + V_{1}^{*}. \quad (9)$$

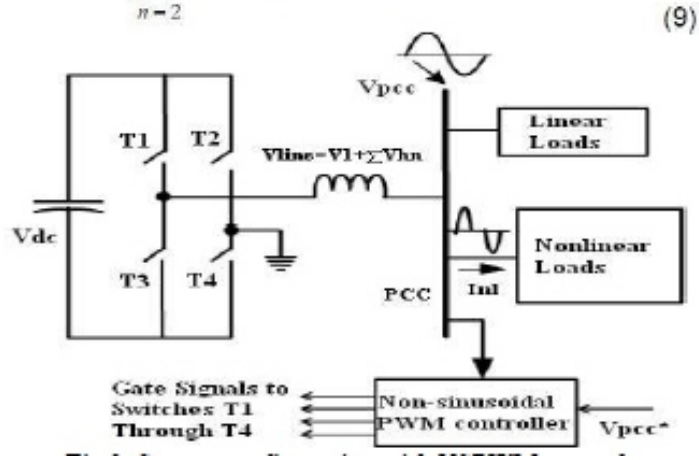

Fig 2: System configuration with NSPWM control

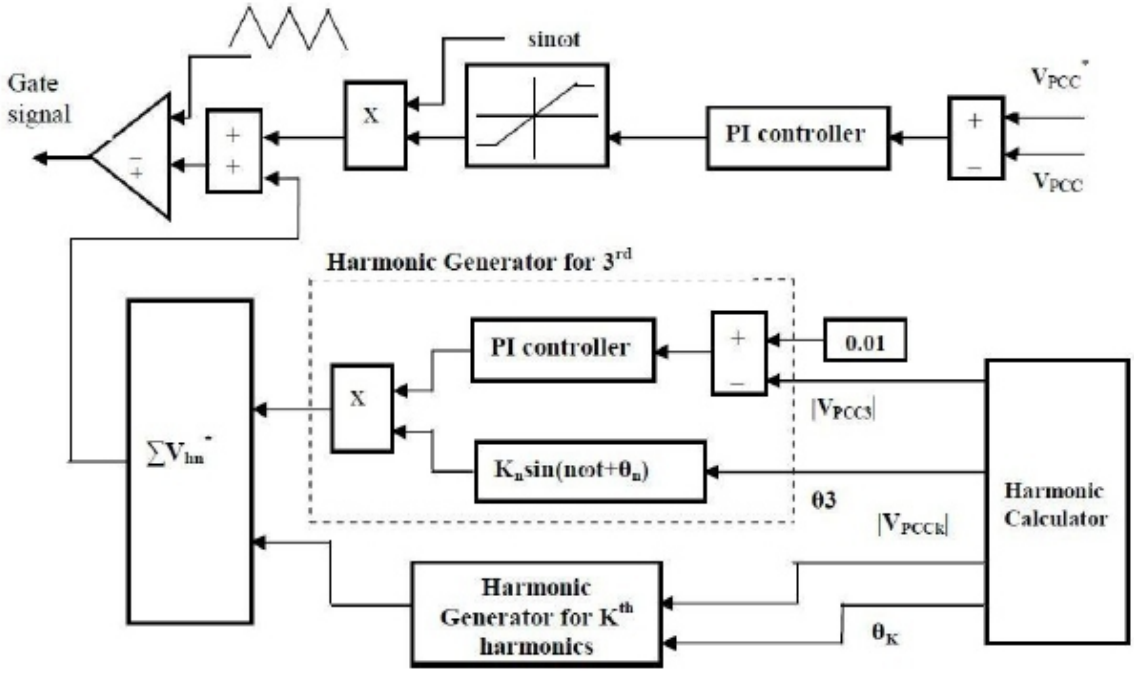

Fig 3: Schematic diagram of the control scheme Generator" blocks. The number of "Harmonic Generator" blocks required depends on the desired

III. CONTROL SCHEME

Fig. 2 shows a single-phase inverter operating in islanded mode and supplying various loads connected at the PCC. Due to the nonlinear current, INL, drawn by the nonlinear loads, becomes nonsinusoidal. The NSPWM controller takes VPCC as the input and generates a nonsinusoidal reference waveform (Vref*) for firing the switches T1 through T4 of the inverter. This nonsinusoidal reference is compared with a triangular waveform to generate PWM signals. The inverter fired with these PWM signals acts as a nonsinusoidal voltage source to produce a desired sinusoidal voltage VPCC* at the PCC. The details of the NSPWM controller block are shown in Fig. 3.

The detailed control scheme, as shown in Fig. 3, consists of two main loops, referred to as the "voltage control loop" and "compensation loop." The voltage- control loop regulates the voltage at the PCC. The PI controller of this loop adjusts the amplitude of the sinusoidal reference waveform and, thus, controls the modulation index as is done in a conventional sinusoidal PWM (SPWM) technique. The compensation loop modulates the sinusoidal reference waveform with the harmonic frequencies present in the load current to generate a nonsinusoidal reference Vref*. This nonsinusoidal reference, as in the case of SPWM, is compared with a repetitive high-frequency triangular waveform.

The controller requires information only about the voltage at the PCC to generate the nonsinusoidal reference waveform discussed before. The magnitude $|VPCCn|$ and the angle θn of each harmonic component, present in VPCC, are derived using "Harmonic Calculator" shown in Fig. 3. This

information is then passed on to the "Harmonic THD in the voltage at the PCC. Fig. 3 shows the "harmonic generator" blocks for 3rd through kth harmonic components. The PI controllers of these harmonic generators adjust the amplitude of the respective reference harmonic components (defined in Section II) into the reference waveform.

The reference value, set for all of these PI controllers should be less than 0.03. Thus, these loops ensure that the individual harmonic components in the voltage at the PCC are brought to the levels recommended by the standards. The error voltage, given by (7), is applied to the individual PI controller whose output is multiplied with the sine wave at the respective harmonic frequency. It is also delayed by an angle identical to that of the phase of that harmonic in the output voltage. This forms the "reference harmonic component" given by (8). Thus, each harmonic block produces its respective harmonic components. The reference harmonic components generated by these "harmonic generator" blocks are added with the sinusoidal reference obtained from the "voltage control" loop to produce a modulated nonsinusoidal reference waveform Vref* given by (9).

IV. SIMULATION RESULTS

The scheme discussed before is simulated with MATLAB/Simulink and the results of the simulation are presented in this section. The loads considered (as an example) for the simulation study are comprised of the following loads

Case 1) Resistive load R1 = 80Ω.

Case 2) Resistive load R1 = 80Ω and parallel combination of R2 = 20Ω and L2 = 8.5mH per phase connected in parallel at the PCC.

Case 3) Resistive load R1 = 80Ω and parallel combination of R2 = 20Ω and L2 = 5.53mH per phase and parallel combination of R3 = 16Ω and C3 = 2.78μF per phase connected in parallel at the PCC.

The input dc supply voltage (Fig. 3) for the simulation is considered to be 200 V. The reference voltage is set at 200 V, to achieve an rms voltage of 200 V at PCC. The DG source is tied to the point of common coupling (PCC) through an inverter and a series inductor having an inductance of 0.12mH and an internal resistance of 0.5mΩ. The series inductor is essential from the control and protection point of view. An isolation transformer is connected in transmission line to block transmission of DC signals from one circuit to the other, but allow AC signals to pass and also block interference caused by ground loops.

The above three cases are simulated in both Sinusoidal Pulse Width Modulation (SPWM) and Non Sinusoidal Pulse Width Modulation (NSPWM) and the results are shown below.

Fig 4 and 5 shows the simulink circuit of the three phase DG source supplying various loads at the PCC under SPWM control and NSPWM control respectively. It shows three different loads connected in parallel. Fig 6 shows the harmonic generator block in which each block represents 3rd, 5th, 7th, 9th, 11th, 13th harmonic blocks respectively. The operation of harmonic generator is explained in section III. Fig 7 shows harmonic calculator block of 3rd harmonic. The block extracts the 3rd harmonic component in the voltage and calculates the magnitude and phase difference.

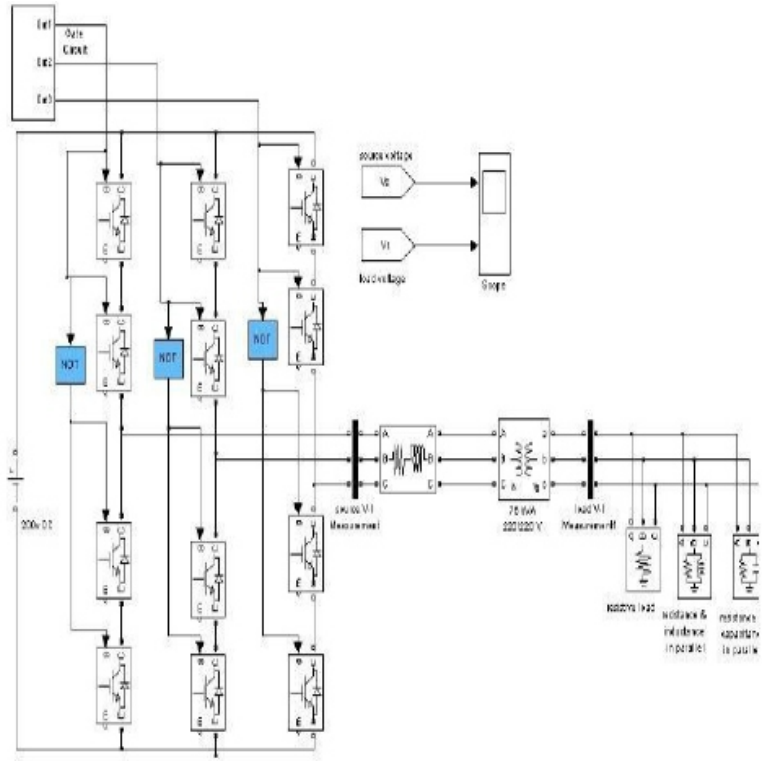

Fig 4: Simulink circuit with SPWM control.

The three different loads as mentioned above are simulated separately with both SPWM control and NSPWM control and are shown below.

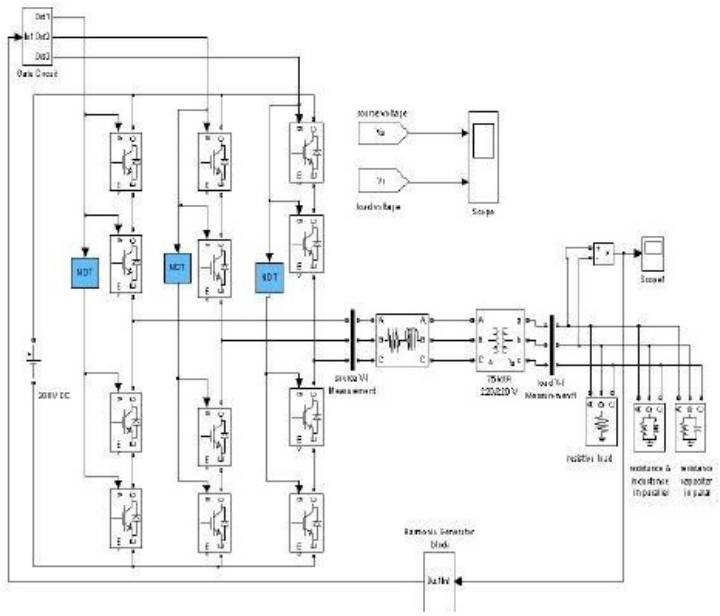

Fig 5: Simulink circuit with NSPWM control.

Case 1:

Fig 8 shows the output voltage of inverter, load voltage under SPWM control and load voltage under NSPWM control. It is clear that under SPWM control the voltage waveform is highly distorted. The NSPWM control gradually modulates the reference waveform by introducing harmonic components into it.

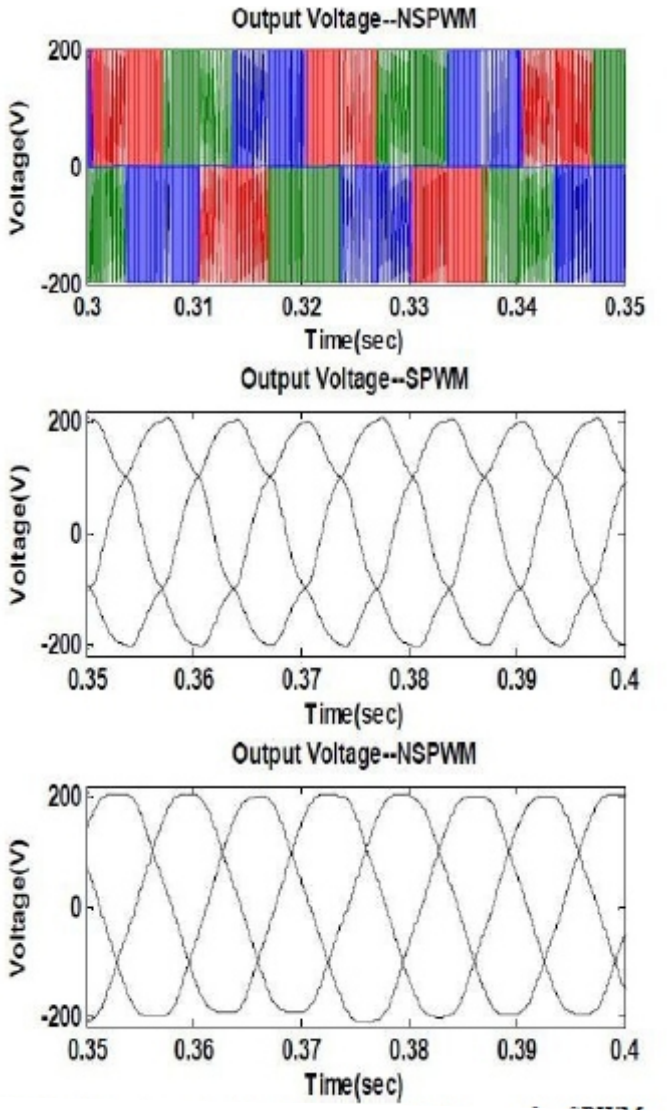

Fig 8: a) inverter output voltage b) load voltage under SPWM control c) load voltage under NSPWM control.

TABLE I Comparison of the harmonic spectrum under SPWM and NSPWM operation (case I)

Order of the harmonics	amplitude of the component	
	With SPWM	With Proposed scheme
3	0.41	0.09
5	10.43	6.04
7	7.72	1.78
9	0.09	0.08
11	0.45	0.4
13	1.14	0.11
15	0.04	0.06
THD	6.82%	3.73%

Shunt compensation has been used in between transmission line with a capacitance of 3μF per phase in order to maintain voltage constant. Table I shows the dominance of 5th and 7th order harmonics with their amplitudes of 10.43 V and 7.72 V. respectively under SPWM control. The THD under these conditions is 6.82%. The dominant harmonics shown above are reduced to 6.04 V and 1.78 V respectively in NSPWM control. The THD under these conditions is 3.73%. It is also observed that the harmonic spectrum of VPCC mainly consists of odd harmonics. The reason for the absence of even harmonics is the quarter-wave symmetry of the load current.

Case 2:

Loads R1 and parallel combination of R2 and L2 connected in parallel at PCC:

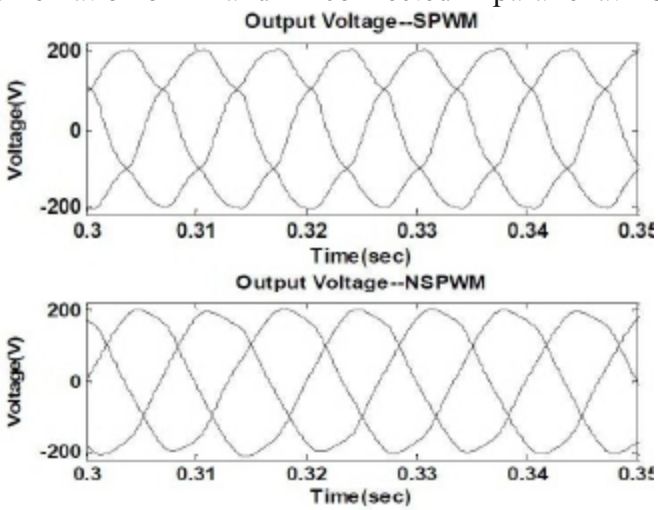

Fig 9: a) load voltage under SPWM control b) load voltage under NSPWM control.

Fig 9 shows the output voltage at PCC under SPWM control and NSPWM control respectively. Where in SPWM control the voltage waveform is distorted, the NSPWM control gradually modulates the reference waveform by introducing harmonic components into it and the distortion is reduced. Here in this case a filter is used in load side in order to reduce the harmonics created by the inductive load. Table II shows the dominance of 5th and 7th order harmonics with their amplitudes of 16.65 V and 9.11 V respectively under SPWM control. The THD under these conditions is 9.84%. The dominant harmonics shown above are reduced to 4.96 V and 1.33 V respectively in NSPWM control. The THD under these conditions is 2.76%.

TABLE II Comparison of the harmonic spectrum under SPWM and NSPWM operation (case II)

Order of the harmonics	amplitude of the component	
	With SPWM	With Proposed
3	0.16	1.24
5	16.65	4.96
7	9.11	1.33
9	0.03	0.31
11	0.58	0.4
13	1.37	0.04
15	0.03	0.14
THD	9.84%	2.76%

Case 3:

Loads R1, parallel combination of R2 and L2 and parallel combination of R3and C3 connected in parallel at PCC:

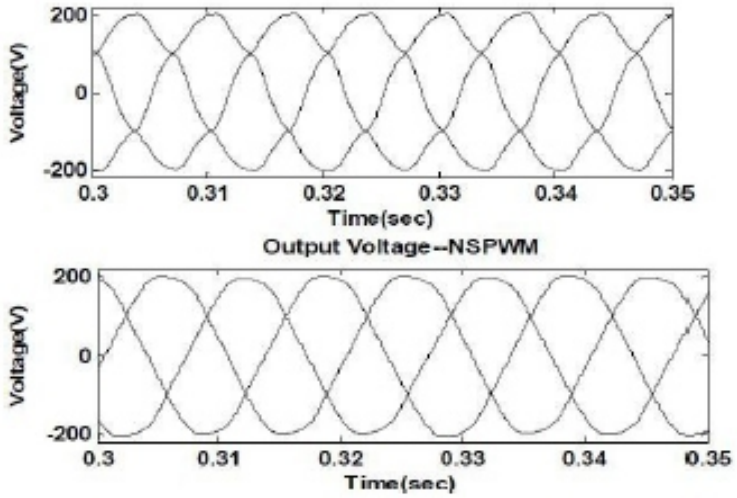

Fig 10: a) load voltage under SPWM control b) load voltage under NSPWM control

Fig 10 shows the output voltage at PCC under SPWM control and NSPWM control respectively. It is clear from fig 10, in SPWM control the voltage waveform is distorted, the NSPWM control gradually modulates the reference waveform by introducing harmonic components into it and the distortion is reduced. Table III shows the dominance of 5th and 7th order harmonics with their amplitudes of 11.6 V and 7.08 V respectively under SPWM control. The THD under these conditions is 7.12%. The dominant harmonics shown above are reduced to 4.31V and 0.77 V respectively in NSPWM control. The THD under these conditions is 2.84%.

TABLE III Comparison of the harmonic spectrum under SPWM and NSPWM operation (case III)

Order of the harmonics	amplitude of the component	
	With SPWM	With Proposed scheme
3	0.08	2.21
5	11.6	4.31
7	7.08	0.77
9	0.04	0.24
11	0.46	0.5
13	1.14	0.25
15	0.03	0.2
THD	**7.12%**	**2.84%**

CONCLUSION

Nonlinear loads connected at the PCC cause a nonlinear drop across the line impedance and, hence, distort the supply voltage available at the PCC. This problem gets more pronounced during islanding. In this paper, a scheme based on the NSPWM technique has been proposed which is capable of compensating the nonsinusoidal drop across the line impedance and producing regulated sinusoidal voltage at the PCC. Not only is the THD reduced, the individual harmonic components are also reduced to a specified level. The only input that the controller requires for its operation is the voltage at the PCC. A notable feature of the proposed algorithm is that it does not require any current sensor or any other external compensating device. Also, it does not require the load and line parameters' values. The THD of the voltage at PCC is dependent on the number of harmonics extracted and introduced into the nonsinusoidal reference waveform. To compensate "n" harmonic components present in the voltage at PCC "n" harmonic generator blocks are required.

However, most of the loads (like the one considered) present quarter-wave symmetry where only odd harmonics are present. Hence, in such cases, the "harmonic generator" blocks are required only for the odd harmonics. This minimizes the number of harmonic generator blocks and reduces the mathematical analysis. The satisfactory performance of the controller is demonstrated using the simulation results obtained in MATLAB/Simulink.

REFERENCES

[1] K. S. Tam and S. Rahman, "System performance improvement provided by a power conditioning subsystem for central station photovoltaic-fuel cell power plant," IEEE Trans. Energy Convers., vol. 3, no. 1, pp. 64–70, Mar. 1988.

[2] M. I. Marei, E. F. El-Saadany, and M. M. A. Salama, "Flexible distributed generation: (FDG)," in Proc. IEEE Power Eng. Soc. Summer Meeting, Jul. 2002, vol. 1, pp. 49–53.

[3] K. Ro and S. Rahman, "Control of grid-connected fuel cell plants for enhancement of power system stability," Renew.

Energy, vol. 28, no. 3, pp. 397–407, Mar. 2003

[4] K. Ro and S. Rahman, "Two-loop controller for maximizing performance of a grid-connected photovoltaic-fuel cell hybrid power plant," IEEE Trans. Energy Convers., vol. 13, no. 3, pp. 276–281, Sep. 1998.

[5] N. Reddy and V. Agarwal, "Utility interactive hybrid distribution generation scheme with compensation features," IEEE Trans. Energy Convers., vol. 22, no. 3, pp. 666–673, Sep. 2007.

[6] F. Katiraei, M. R. Iravani, and P. W. Lehn, "Micro-grid autonomous operation during and subsequent to islanding process," IEEE Trans. Power Del., vol. 20, no. 1, pp. 248– 257, Jan. 2005.

[7] T. Kawabata and S. Highashino, "Parallel operation of voltage source inverters," IEEE Trans. Ind. Appl., vol. 24, no. 2, pp. 281–287, Mar. 1988.

[8] T. Ackermann and V. Knayzkin, "Interaction between distributed generation and the distribution network: Operation aspects," in Proc.Power Eng. Soc. Transmission Distribution Conf., Oct. 2002, vol. 2,pp. 1357–1362.

[9] V. E.Wagner, J. C. Balda, D. C. Griffith, A. Mc-Eachern, T. M. Barnes, D. P. Hartmann, D. J. Phileggi, A. E. Emannuel, W. F. Horton, W. E. Reid, R. J. Ferraro, and W. T. Jewell, "Effect of harmonics on equipment," IEEE Trans. Power Del., vol. 8, no 2, pp. 672–680, Apr. 1993.

[10] F. Z. Peng, "Applications issues of active power filters," IEEE Ind.Appl. Mag., vol. 4, no. 5, pp. 21–30, Sep. 1998.

[11] J. Perez, V. Cardenas, F. Pazos, and S. Ramirez, "Voltage harmonic cancellation in single phase systems using a series active filter with a low-order controller," in Proc. IEEE Power Electronics Congr., Oct. 2002, pp. 270–274.

[12] F. Z. Peng, H. Akagi, and A. Nabae, "New approach to harmonic compensation in power systems-a combined system of shunt passive and series active filters," IEEE Trans. Ind. Appl., vol. 26, no. 6, pp. 983–990, Nov./Dec. 1990.

[13] Z. Wang, O. Wang, W. Yao, and J. Liu, "A series active power filter adopting hybrid control approach," IEEE Trans. Power Electron., vol. 16, no. 3, pp. 301–310, May 2001.

High Performance Portable Charger Using Low- Power PV System

[1]Sangita Mishra, [2]Manoj Kumar Swain
[1]M.Tech. Student (PE&D), GIET, Gunupur, Odisha, India
[2]Asst. Prof, EEE Department, GIET, Gunupur, Odisha, India

ABSTRACT

— This paper proposes an efficient design for a solar-powered charger for low-power devices. The level of the charging current is controllable and any residue power is saveable to a rechargeable 9V battery. Two power sources (AC and solar) are used, and two charging speeds are possible. Quick charging is 20% of the battery output current (almost 180mA/hr) so the current is limited to 34 mA. Two types of cellular batteries (5.7V and 3.7V) can be charged. Normal charging is 10% of the cellular battery output current (almost 1,000mA/hr), so the charging current is limited to 100mA. The design uses only a few components so the system is cost effective besides being highly portable. It was simulated on MultiSim Ver. 11 before being implemented practically to validate it. The results from the simulation and the experiment show the design's sufficient feasibility for practical implementation.

Keywords— PV Energy System, Portable Charger, Current Limiting.

I. INTRODUCTION

The emergence of alternative energy sources and new forms of exploration will rise with the technological evolution and development of societies. In the Eighteenth Century with rudimentary technology there was renewable energy. At the First Industrial Revolution, was the discovery of coal associated with the steam machine? In the Nineteenth Century is the World War I with the discovery of the principles of thermodynamics, development of transport, discovery of oil and natural gas in the Mid-twentieth Century. With World War II, nuclear power appears later computer science, robotics, which together gives rise to the Third Industrial Revolution in the last decades of the twentieth century [1-3].

In the recent past, many countries have strengthened their efforts to increase the fraction of electricity produced from renewable energy sources in order to reduce the greenhouse gas emissions from fossil fuel power plants. While most modern electrical appliances receive their power directly from the utility grid, a growing number of everyday devices require electrical power from batteries in order to achieve greater mobility and convenience. Rechargeable batteries store electricity from the grid for later use and can be conveniently recharged when their energy has been drained. Appliances that use rechargeable batteries include everything from low-power cell phones to high- power industrial fork lifts. The sales volume of such products has increased dramatically in the past decade [4-6].

The system used to draw energy from the grid, store it in a battery, and release it to power a device is called a battery charger system. While designers of battery charger systems often maximize the energy efficiency of their devices to ensure long operation times between charging, they often ignore how much energy is consumed in the process of converting ac electricity from the utility grid into dc electricity stored in the battery. Significant energy savings are possible by reducing the conversion losses associated with charging batteries in battery- powered products [3].

Mobility and mobile computing systems are systems that can easily be physically moved or may be performed while being moved. The small size, limited memory and processing power, low power consumption and limited connectivity are the main characteristics of mobile devices.

The reliance on small devices and the ones which makes easier the daily tasks increases every day. With advances in solar technology, batteries and electronics in general, have been increasingly possible to develop new devices that require less energy to operate. Of course all mobile devices (without network connection) could have, because the power required for solar modules is suitable for battery use. Furthermore, mini charge regulators that reach the maximum power devices without causing overload of the batteries.

Portable devices (mobile phones, tablets, notebooks and netbooks) have become increasingly popular, especially with the proliferation of access to wireless technology. One of its main characteristics is to rely on battery power for its operations. Techniques that allow energy savings, therefore, have been researched to meet the need for immediacy in which the world currently requires [3].

Batteries are nowadays the main energy provider to portable devices. They are used for their high power density and ease of use. Their disadvantages, however, limit their application. Their energy density can drop to as low as 200Wh/kg and their technology seem to improve slower than do other technologies [5-8].

Depleting fossil fuel and increased demand for energy have spurred the search for other sources of energy such as solar, wind, ocean thermal, tidal, biomass,geothermal, nuclear energy, etc. The abundance and widespread availability of solar energy, however, make it the most attractive among other energies that can be feasibly extracted. It can be converted into electricity through low-power PV energy systems, for portable applications (charging of mobile phones) and used in rural areas (solar lamps). The high cost of PV panels and their low efficiency, however, reduce solar energy's competitiveness in the energy market as a major source of power generation. It still, however, is better than conventional energy sources where portability is required [9-12].

This paper considers a novel design for, and the physical implementation of, a solar-charger-based PV energy system for charging of cellular and rechargeable batteries. The charger current can be controlled and any residue power saved in a rechargeable battery (9V). Sources for the design are a solar panel (3W, 18V) and an AC power supply. Two charging speeds are possible (slow and fast). The paper next presents the design of the novel system and its simulation, the experiment results, and the practical implementation [13-16].

II. BATTERY CHARGING:

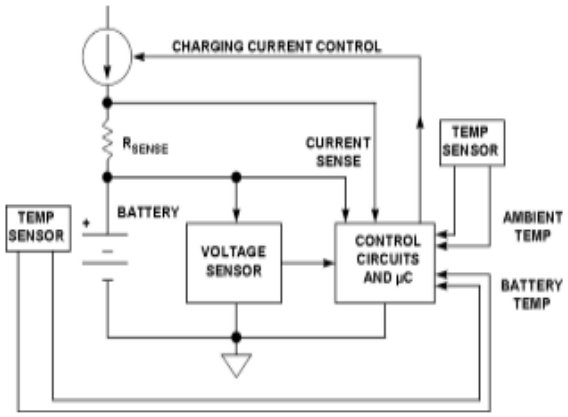

Fig. 1. Generalized Battery Charging Circuit[6]

A generalized battery charging circuit is shown in Fig. 1. The battery is charged with a constant current until fully charged. The voltage developed across the RSENSE resistor is used to maintain the constant current. The voltage is continuously monitored, and the entire operation is under the control of a microcontroller which may even have an on-chip A/D converter. Temperature sensors are used to monitor battery temperature and sometimes ambient temperature.

This type of circuit represents a high level of sophistication and is primarily used in fast- charging applications, where the charge time is less than 3 hours. Voltage and sometimes temperature monitoring is required to accurately determine the state of the battery and the end-of- charge. Slow charging (charge time greater than 12 hours) requires much less sophistication and can be accomplished using a simple current source.

III. NOVEL DESIGN OF THE SOLAR- POWERED PORTABLE CHARGER WITH CURRENT LIMITER

Fig. 2 is a block diagram of the proposed charger. The solar and dc power sources join through two decoupling diodes. The meeting point provides the dc supply voltage to the main part of the design, which has two charging circuits of different specifications. One charging circuit delivers suitable voltage and (limited) charging current to a rechargeable battery, whereas the other is for charging of two types of mobile devices (3.7V and 5.7V).

In general the battery chargers operate in three modes:

1. Active charge mode, during which the battery is being charged from a discharged state. Most battery chargers draw the most power from the outlet during this mode.

2. Maintenance charge mode, during which the battery charge state is being maintained at a fully-charged state. A battery charger typically draws less power in this mode than in active charge mode.

3. No battery mode, during which no battery is connected to the charger at all. Many chargers continue to draw a current in this mode, even though they are doing no useful work [5,6].

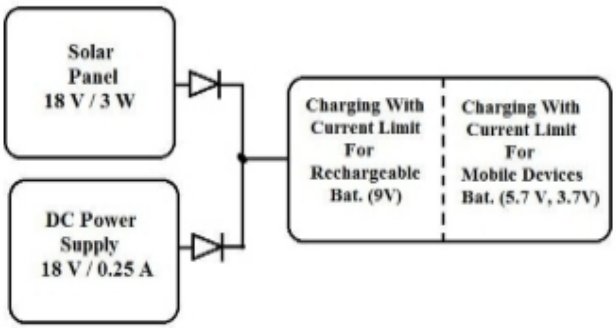

Fig. 2. The proposed portable charger

DC Power Supply Circuit

Fig. 3 shows an 18V/250mA dc power source supplying two successive charging circuits. The power supply circuit is a full-wave rectifier with a step-down transformer (T1: 220 / 15V, 250mA).

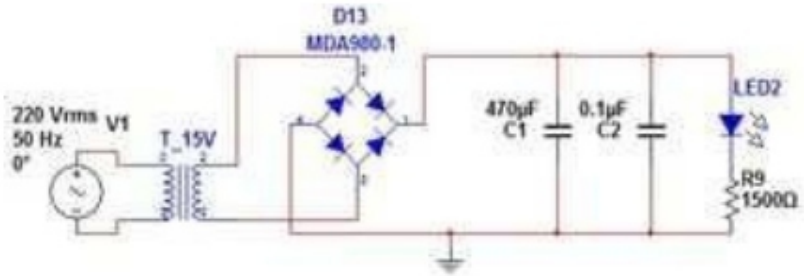

Fig. 3. The 18V / 0.25A, DC Power Supply

Charging with the Current Limiter Circuit

The circuit delivers the higher power supply between the two to the next part of the circuit. Its second function is to provide a suitable charging voltage to a 9V rechargeable battery and supply a high level of charging current (20% of the battery output current, i.e., almost 180mA/hr, so the proposed design limits the current to 34mA, for which the shunt resistor controlling the charging limit should be R3=20Ω. The maximum voltage Vbe must be 0.7V. Of the transistor, R3 = Rbe = (0.7V / 34mA) = 20.5Ω. The second part of the circuit provides charging voltages to 5.7V and 3.7V cellular batteries during suitable selection of the Zener diode connections D2 (ZDP7.5) and D6 (ZDP6.2), also supplies 100mA of charging current when the shunt resistor (R6, 7Ω) is connected (see Fig.4).

The current-limiting action is effected from measuring the current that passes through the shunt resistor. If it reaches the value lead to the voltage across the base and emitter equal 0.7V in will effect directly on the load voltage to make continuous current control on the load current (Charging Current), this action was done for 9V rechargeable battery during transistors Q1 and Q3. The same was done for cellular battery, with transistor Q4 and Darlington transistors Q9 and Q10. Fig. 3 is the proposed practical electronic circuit and all the distributed meters for the complete simulated measurements.

IV. SIMULATION RESULTS

The secondary coil of the stepdown transformer provided 15Vac, the load current was 124.79mA, the load resistance was 150Ω, and the dc load voltage was 18.7V; all these were measured by the third meter. The dc power supply delivered the required load currents in normal charging of rechargeable battery and cellular device.

- **The Complete Charging Circuit with Current Limiter**

Fig. 5 shows the complete simulations for the proposed charger. One is for rechargeable-battery charging current limited to 34mA (high-speed charging level), the other for cellular-battery charging current limited to 100mA (normal level). Calculations for the charging current levels were based on these: base emitter resistor R3=0.7V for transistor Q3 forward voltage (limiting to 34mA the rechargeable battery charging current). The value for a suitable base resistor will thus depend on the following: R(be) = Vbe / I(pass through Rbe). The maximum value for Vbe was limited to 0.7V. After correct selection of the current to pass through the resistor (for rechargeable battery, we selected the current level to equal the high-speed charging limit of 34 mA), a suitable resistor value would be Rbe = Vbe / Ibe = (0.7V) / (34mA) = 20.5Ω.

Through the same procedure but for different levels of charging current, the resistor selected to limit the maximum charging current was 7Ω. Fig. 5 include all related records as a drawings data came from distributed multimeters, the reads cover different case with suitable range of dc input voltage which came from the meeting point of diodes connection of the switching supply and DC power supply, from data and the related drawing in the Fig. 4 that fixed zeners voltages for range of Vdc input, It explains the charging current level around the current value of 34mA for rechargeable battery, and It explains the controlling of the level of charging current came from the designed value of resistor and the effect of the base emitter voltage, by same principle the recorded data of the charging current (XMM8) in mobile devices battery not pass more than 100mA.

V. IMPLEMENTING THE DESIGN

The design is a PV-based (3W, 18V) energy system for mobile applications. It contains a PV array, a circuit design model, an oscilloscope, and a 9V DC battery for charging (see Fig. 5). After full charging, the battery starts converting energy through the 9V DC battery (which is used when the solar source dries up or at night). Control of the battery charging involves maintaining the current level at the high-speed charging limit equaling 34mA.

Fig. 6. Practical Implement of System Design and Final Product Form.

Different levels of charging current are possible (the normal charging level is 100mA). The rechargeable battery was charged to 34mA and the results fully correspond with the simulation results.

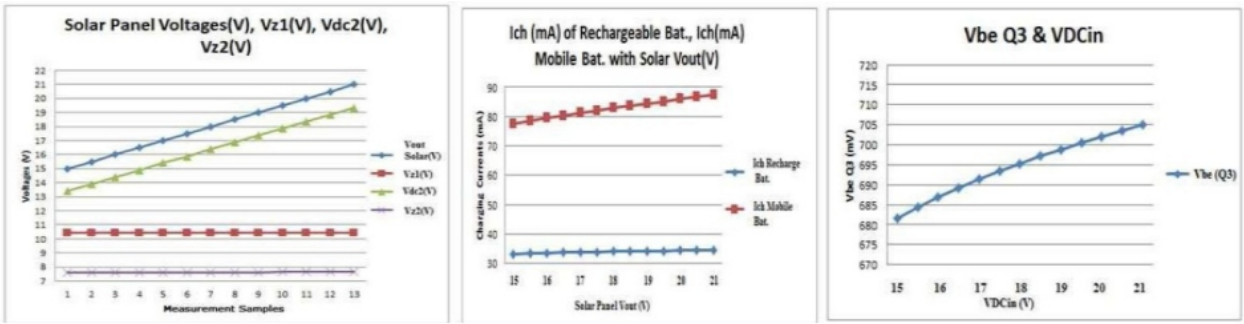

(Fig. 5. Simulation Data for the Charging Circuit, the Charging Current, and the Controlling Voltage)

Fig. 6 also shows the final display of the mobile charger. The selection for the source type (either solar energy or AC) depends on the source available. The level of charging of the external battery also shows up on the panel.

CONCLUSION

The proposed design is novel. It is simple and cheap but high performance. It also functions on two sources. Its simulation and experiment results show: Above 95% charging efficiency (proving solar energy's feasibility in supplying energy to mobile phones).

Its current limiter circuit extending battery life and it is safe even after full charging. Possible future work in increasing the solar panel efficacy and reducing the system size.

REFERENCE

[1] *Attia H. A, Getu B, Ghadban H, Abu Mustafa K, Portable Solar Charger with Controlled Charging Current for Mobile Phone Devices, Int. J. of Thermal & Environmental Engineering, Vol. 7, No. 1, 2014 , pp.17- 24*

[2] *Hild S, Leavey S, Sorazu B, Smart Charging Technologies for Portable Electronic Devices, Journal Of Latex Class Files, 2014.*

[3] *Geist T, Kamath H, Porter S, Designing Battery Charger Systems for Improved Energy Efficiency, Prepared for the California Energy Commission, Sep 28, 2006.*

[4] *F. Boico, B. Lehman, Multiple-input Maximum Power Point Tracking algorithm for solar panels with reduced sensing circuitry for portable applications, J. Solar Energy 86 (2012) 463–475*

[5] *P. Görbe , A. Magyar, K. M. Hangos, Reduction of power losses with smart grids fueled with renewable sources and applying EV batteries, J. Cleaner Production 34 (2012) 125-137*

[6] *P. Bajpai, V. Dash, Hybrid renewable energy systems for power generation in stand-alone applications: A review, J. Renewable and Sustainable Energy Reviews 16 (2012) 2926–2939*

[7] *B. ChittiBabu, et. al, Synchronous Buck Converter based PV Energy System for Portable Applications, Proceeding of the 2011 IEEE Students' Technology Symposium 14-16 Jan. (2011), 335 - 340*

[8] *A. Robion, et. al, Breakthrough in Energy Generation forMobile or Portable Devices, 978-1- 4244-1628-8/07/$25.00©2007 IEEE, (2007),*

[9] *M. H. Imtiaz, et. al, Design & Implementation Of An Intelligent Solar Hybrid Inverter In Grid Oriented System For Utilizing PV Energy, International Journal Of Engineering Science And Technology, Vol. 2(12), 2010, 7524-7530*

[10] *M. S. Varadarajan, Coin Based Universal Mobile Battery Charger, IOSR Journal of Engineering (IOSRJEN) ISSN: 2250-3021 Vol. 2, Issue 6 (June 2012), 1433-1438*

[11] *R. M. Akhimullah, Battery Charger with Alarm Application, Thesis of Bachelor Of Electrical Engineering (Power System), University Malaysia Pahang, November, 2008, pp: 1-24*

[12] *M. A. Baharin, Solar Bicycle, thesis MSc. Bachelor Of Electrical Engineering (Power Systems), University Malaysia Pahang, November, 2010, pp:1-24*

[13] *J. Tyner, et. al, The Design of a Portable and Deployable Solar Energy System for Deployed Military Applications, Proceedings of the 2011 IEEE Systems and Information Engineering Design Symposium, University of Virginia, Charlottesville, VA, USA, April 29, (2011), 50 - 53*

[14] *C. Li, et. al, Solar Cell Phone Charger Performance in Indoor Environment, 978-1-61284-8928-0/11/$26.00 ©2011 IEEE, (2011), pp: 1-2.*

[15] *Q. I. Ali, Design & Implementation of a Mobile Phone Charging System Based on Solar Energy Harvesting, Iraq J. Electrical and Electronic Engineering, Vol.7 No.1,(2011), 69 -72*

[16] *K. Ishaque, Z. Salam, A review of maximum power point tracking techniques of PV system for uniform insolation and partial shading condition, J. Renewable and Sustainable Energy Reviews, 19, (2013), 475–488.*

[17] *A. Higier, Design, development and deployment of a hybrid renewable energy powered mobile medical clinic with automated modular control system, J. Renewable Energy ,50, (2013), 847 - 857*

[18] *M.H. Taghvaee, et. al, A current and future study on non- isolated DC–DC converters for photo voltaic applications, J. Renewable and Sustainable Energy Reviews, 17, (2013) 216–227*

[19] *R. Komiyama, Analysis of Possible Introduction of PV Systems Considering Output Power Fluctuations and Battery Technology, Employing an Optimal Power Generation Mix Model, Electrical Engineering in Japan, Vol. 182, No. 2, (2013), pp. 1705–1.*

LLC Resonant Inverterfor Solar PV Applications

[1]Kirlampalli Harija Rani, [2]Ch Venkateswara Rao
Department of Electrical Engineering, Raghu Institute of Technology, Visakhapatnam, India
Department of Electrical& Electronics Engineering, GIET, Gunupur, India
E-mail: 1harijarani.69@gmail.com

A B S T R A C T

— In this paper, a high-efficiency solar array simulator (SAS) implemented by an LLC resonant dc–dc converter is proposed to save the cost and energy of photovoltaic (PV) system testing. The proposed converter has zero-voltage switching (ZVS) operation of the primary switches and zero-current switching (ZCS) operation of the rectifier diodes. The output impedance of LLC resonant converter can be regulated from zero to infinite value by frequency modulation control and without shunt or serial resistors. Therefore, the efficiency of the proposed SAS can be significantly increased. The circuit operations are analyzed in detail to derive the theoretical equations. Circuit parameters are designed based on the practical considerations. Finally, an illustrative example is implemented to demonstrate the feasibility of the proposed SAS.

Keywords—LLC resonant dc–dc converter, photovoltaic (PV)system, solar array simulator (SAS)

I. INTRODUCTION

The Resonant switching topology is one of the most efficient solutions for switch mode power supply Design (SMPS). LLC resonant converter in its half- bridge configuration gained more popularity than the other. High efficiency, High power density and high power are the major driving force for this research work.

The ultimate target is to find a topology, which could be optimized at high input voltage with low switching loss.To limit all these issues, a topology competent of higher switching frequency with higher efficiency is the means to achieve the goal[1]. By using proposed techniques in this paper, the performance of the system under normal operation could be improved. But in power electronics none of the methods dealt with the switching loss problem of PWM converter. Even Zero Voltage Switching (ZVS) technique minimize the loss during turn-on but unable to limit turn-off loss which leads to failure of converter operation at higher switching frequency[2].

Fundamentally, resonant converter is a switching converter that includes a tank circuit dynamically participating in determining the power flow between input and output. High switching frequency operation is possible with resonant converters due to their low switching loss. In resonant converters,Series Resonant Converter (SRC),Parallel Resonant Converter (PRC) and Series Parallel Resonant Converter (SPRC, also called LCC resonant converter) are the three most popular topologies.

II. LLC RESONANT CONVERTER

Circulating currents and switching loss becomes more at high input voltage in existing converters like SRC, PRC and SPRC [3]. So they are not suitable for front end DC/DC application. LCC resonant converter also could not be optimized for high input voltage range. The reason is same for SRC,PRCand LCC; the converter switching frequency shifting with rise in input. DC characteristic of LCC resonant converter shown in Fig 2, it can be seen that there are two resonant frequencies. Low resonant frequency is determined by series resonant tank Lr and Csand high resonant frequency determined by Lr and equivalent capacitance of Cs and Cp in series. For a resonant converter, the converter could reach high efficiency at resonant frequency. Even LCC resonant converter has two resonant frequencies but unfortunately, the lower resonant frequency is in ZCS region [4]. Hence for this application, it is not possible to design the converter working at this resonant frequency. By changing the LCC resonant tank to LLC resonant network, this is feasible. As shown in Figure 1, a LLC resonant converter built by changing L to C and C to L. The DC characteristics of these two converters (LCC & LLC)are shown in Figure 2 and Figure3 respectively [5]. We can observe the higher resonant frequency is in the ZVS region, meant that the converter is designed to operate around this frequency.

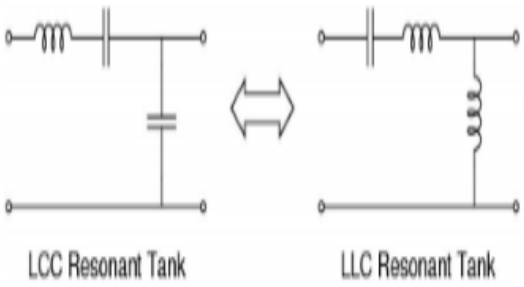

Fig. 1. LCC and LLC resonant Tank

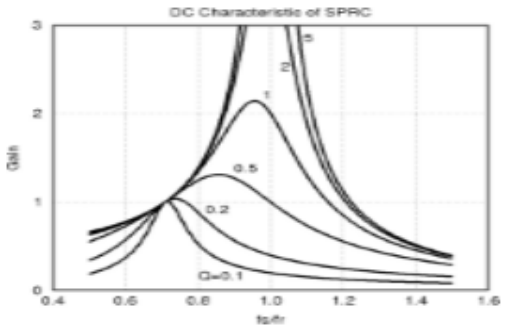

Fig. 2. DC characteristics of LCC resonant converter

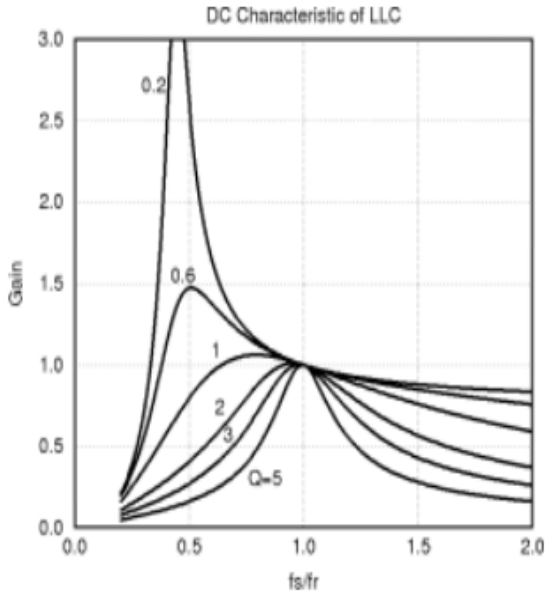

Fig. 3. DC Characteristics of LLC Resonant Converter

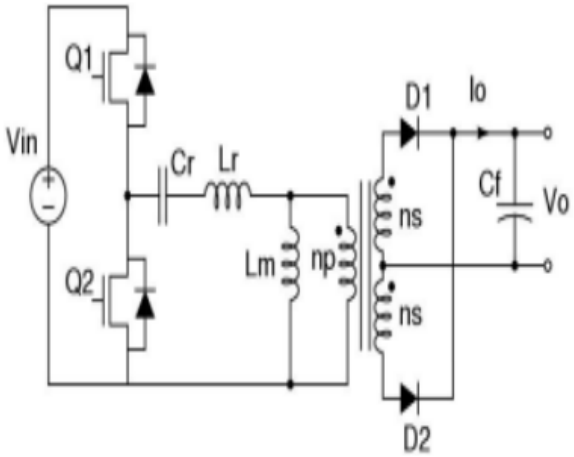

Fig. 4.Half Bridge LLC Resonant Converter

The benefit of LLC resonant converter is ZVS capability under no-load condition and narrow switching frequency range with light load.

In this paper some unfamiliar operating regions of LLC resonant converter was investigated and found very special characteristic in those regions and makes it an excellent option for front end DC/DC application.

III. OPERATION OF LLC RESONANT CONVERTER

The entire DC characteristic of LLC resonant converter divided into two regions i.e. ZVS region and ZCS region as shown in Figure 5[6]. For this converter, there are two resonant frequencies. One frequency is determined by Lr and Cr and other one is determined by Lm, Cr. As load on converter increasing, the resonant frequency will shift towards higher frequency.

$$fr_1 = \frac{1}{2 \cdot \Pi \sqrt{L_r \cdot C_r}} \quad (1)$$

$$fr_2 = \frac{1}{2 \cdot \Pi \sqrt{(L_m + L_r) \cdot C_r}} \quad (2)$$

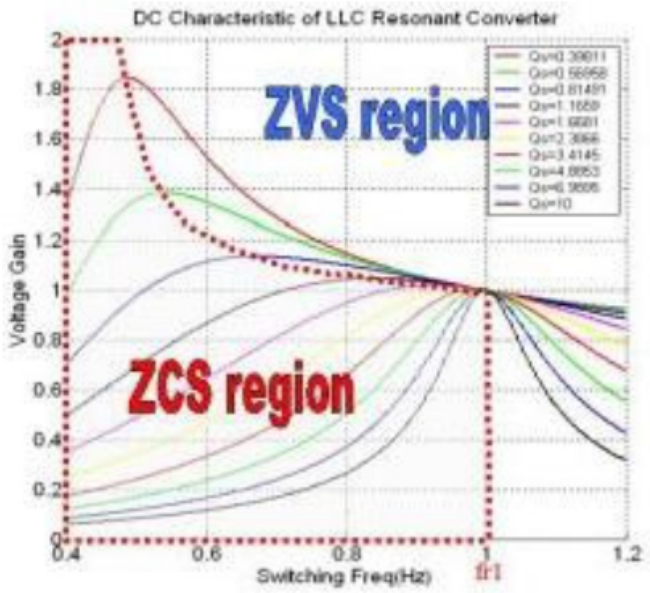

Fig. 5. DC characteristic of LLC resonant converter

A mode of Operation of LLC Resonant Converter is as follows:

Mode 1:

This mode of operation begins when Q2 is turned off at time assume t0. At this instant, current through resonant inductor Lr is negative [7]; it will flow through the switch Q1, that current creates a ZVS condition for Q1. Q1 should be turn-on during this mode.

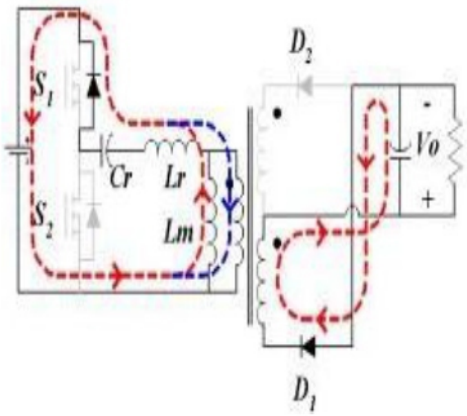

Fig. 6. Circuit Diagram during Mode-1

When the negative current of resonant inductor Lr flow through body diode of Q1, ILr begins to rise, this will cause secondary diode D1to conduct and Io begin to increase [8]. Also, from this instant, transformer secondary winding Lm starts charging with constant voltage.

Mode 2:

Mode-2 begins when current through the resonant inductor ILris positive. Since Q1 is turned on during mode 1, current flow through MOSFET Q1. Output rectifier diode D1starts conduction during this mode. The transformer voltage is clamped at voltage across output capacitor and inductor Lm is linearly charged with output voltage, so it doesn't participate in the resonance during this period [9]. When Lr current is equal to Lm current then this mode ends.

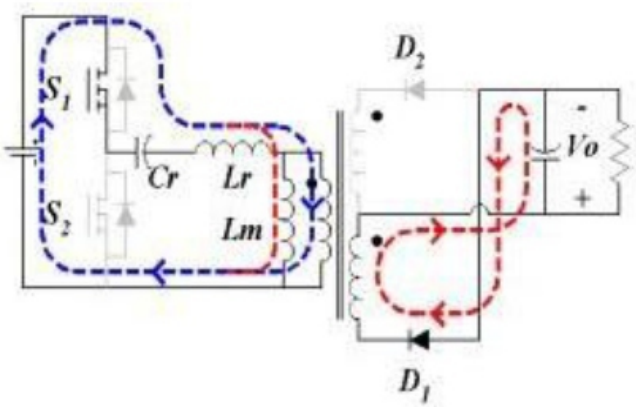

Fig. 7. Circuit Diagram during Mode-2

Mode 3:

At certain instant t2, the two inductor's currents are equal and output current reaches zero amps. Output rectifier diodes D1 and D2 are reverse biased. Reflected voltage due to transformer primary i.e. Transformer secondary voltage is lower than output voltage [10]. During this time, since converter output is separated from transformer primary, Lm is freed to participate resonant. A resonant tank will form with Lm in series with Lr resonant with Cr. When Q1 is turned off then the mode of operation ends . For next half cycle, again mode-1 starts.

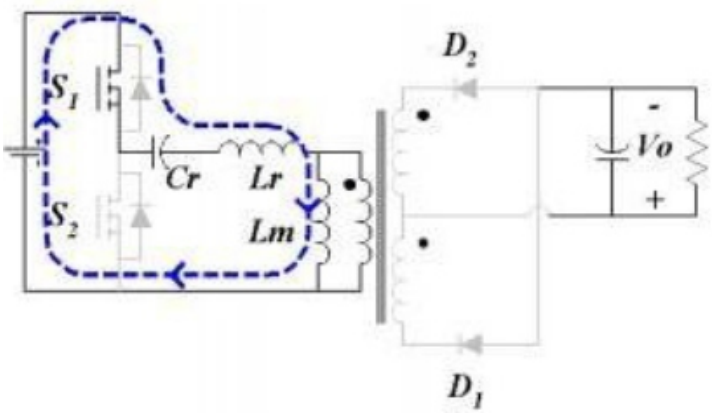

Fig. 8.Circuit Diagram during Mode-3

DESIGN OF LLC RESONANT CONVERTER

The DC characteristic of LLC resonant converter could be derived from above analysis. Based on the DC characteristic, parameters in power stage can be designed [12].

The parameters need to be designed are:

- Transformer turns ratio: n
- Series resonant inductor: Lr
- Resonant capacitor: Cr
- Resonant inductor ratio: Lm/Lr
- The specifications for the design are:
- Input voltage range from 500Vdc
- Output voltage is 28Vdc
- Maximum load about 2.5Ohm
- Maximum switching frequency of operation is 5KHz-100KHz

The transformer turns ratio can be choose based on following equations:

$$n = V_{in}/(2 \cdot V_0) \qquad (3)$$

For Full Bridge LLC resonant converter, the turn's ratio becomes:

$$n = V_{in}/V_0 \qquad (4)$$

In this design, a half bridge LLC resonant converter is used; so the turn's ratio is choosing to be 4.

I. TEST RESULTS

Simulation was carried out to test the functionality of converter for wide range of inputs. The gate voltages of switches with 1V amplitude and also carrier signal been shown here.

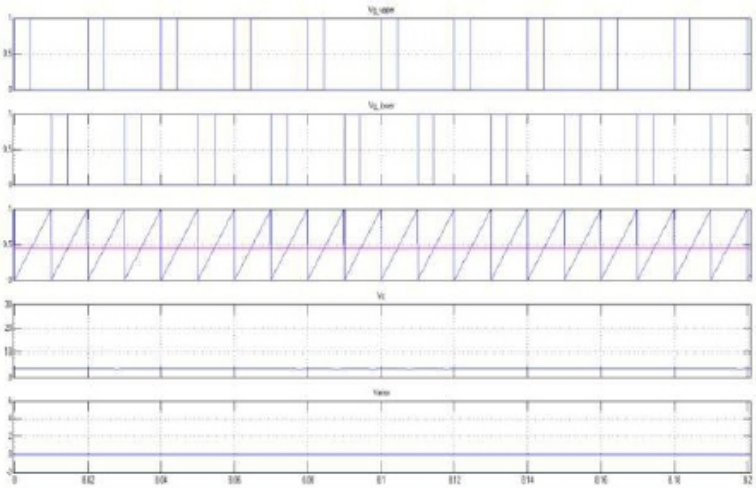

Fig. 9. Controller and gate voltage Waveforms

Input voltage of magnitude 500V and current of 13A has been observed here.

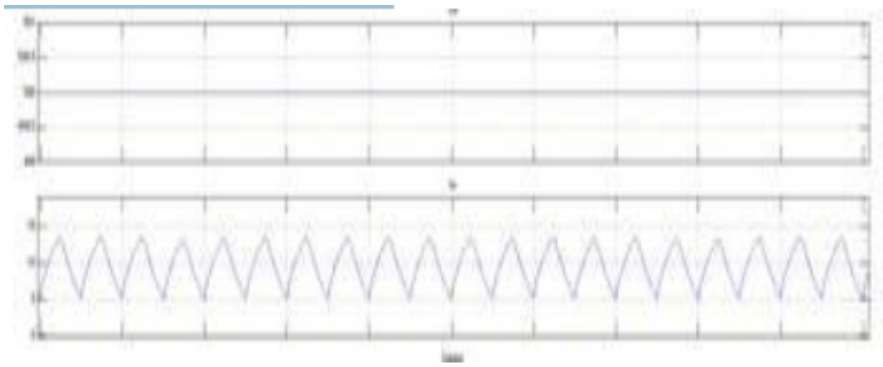

Fig. 10. Input voltage current waveforms

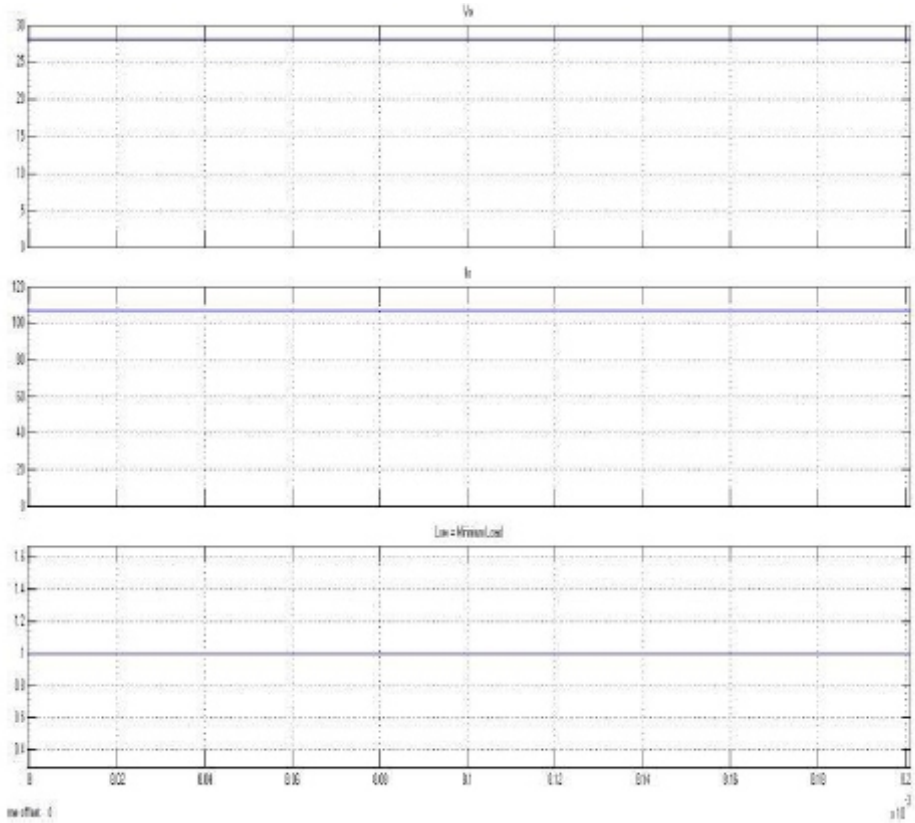

Fig. 11. Output voltage and Current Waveforms

A special type of controller [15] (PIID) has been designed for this application to get 12degrees phase margin. Bode plot of controller with compensated and uncompensated controller shown below.

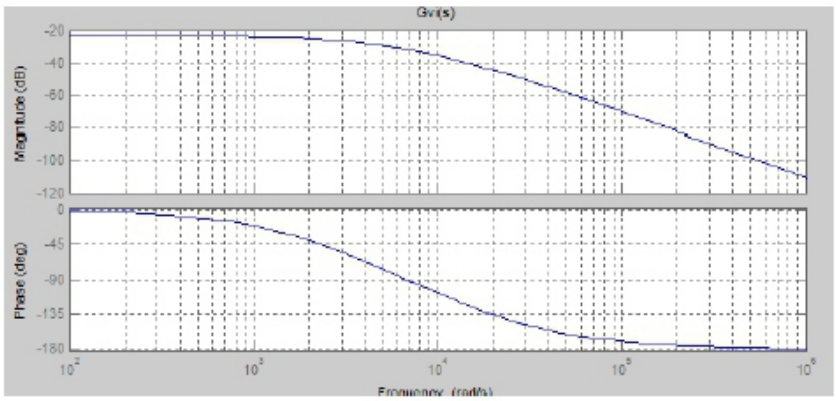

(a)

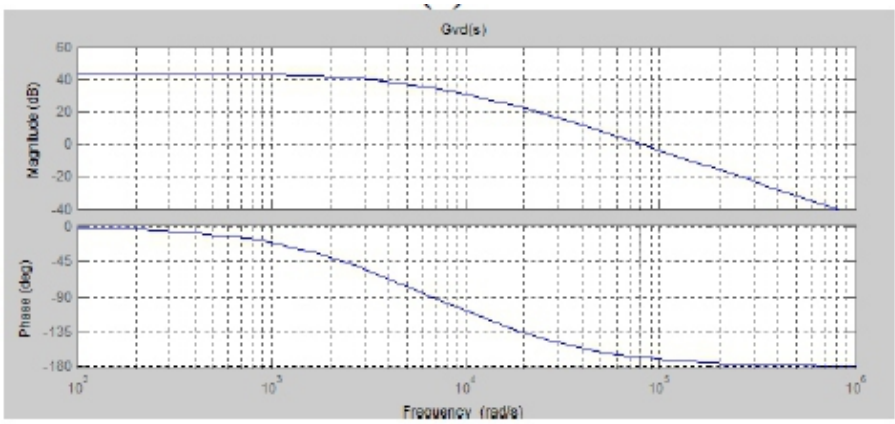

(b)

Fig. 13. (a), (b). Compensator Loop Bode Plot

FUTURE SCOPE

The advantage of LLC resonant converter is that it has two resonant frequencies and the operating point of normal operating condition is positioned at resonant frequency [17]. If we take three elements resonant tanks, there are 36 different configurations. If any other resonant tank configuration is used in the circuit that configuration should provide similar characteristic so that it could result similar benefits.

CONCLUSION:

A high-efficiency SAS implemented by an LLC resonant converter with ZVS feature has been proposed. The detail operation principle, design procedures, and considerations are introduced. A prototype SAS is implemented to demonstrate the feasibility and validity of the theoretical discussion. The experimental results show that the SAS can provide approximated PV output characteristics with high accuracy, and the maximum system efficiency at the range near MPP is up to around 92.5%. Hence, the proposed SAS based on an LLC resonant converter can significantly save the costs and energy for PV system testing, and accelerate the industrial developments of PV power.

REFERENCES

[1] N. Femia, G. Petrone, G. Spagnuolo, and M. Vitelli, "Optimization of perturb and observe maximum power point tracking method," IEEE Trans.Power Electron., vol. 20, no. 4, pp. 963–973, Jul. 2005.

[2] A. K. Abdelsalam, A. M. Massoud, S. Ahmed, and P. N. Enjeti, "High-performance adaptive perturb and observe MPPT technique for Photovoltaic-basedmicrogrids," IEEE Trans. Power Electron., vol. 26, no. 4, pp. 1010–1021, Apr. 2011.

[3] F. Nagamine, R. Shimokawa, M. Suzuki, and T. Abe, "Newsolar simulator for multi-junction solar cell measurements," in Proc. Conf. Rec. 23rd IEEE Photovoltaic Spec. Conf., May 1993, pp. 686–690.

[4] S. Techajunta, S. Chirarattananon, and R. H. B. Exell, "Experiments in a solar simulator on solid desiccant regeneration and air dehumidification for air conditioning in a tropical humid climate," Renewable Energy, vol. 17, no. 4, pp. 549–568, Aug. 1999.

[5] A. K. Mukerjee and N. Dasgupta, "DC power supply used as photovoltaic simulator for testing MPPT algorithms," Renewable Energy, vol. 32,no. 4, pp. 587–592, Apr. 2007.

[6] L. A. C. Lopes and A.-M.Lienhardt, "A simplified nonlinear power source for simulating PV panels," in Proc. IEEE Power Electron. Spec. Conf.,Jun. 2003, pp. 1729–1734.
[7] H. Nagayoshi, "I-V curve simulation by multi-module simulator using I-V magnifier circuit," Solar Energy Mater. Solar Cells, vol. 82, no. 1–2, pp. 159–167, May 2004.
[8] K. Khouzam and K. Hoffman, "Real-time simulation of photovoltaic modules," Solar Energy, vol. 56, no. 6, pp. 521–526, Jun. 1996.
[9] J.-H. Yoo, J.-S.Gho, and G.-H. Choe, "Analysis and control of PWM converter with V-I output characteristics of solar cell," in Proc. IEEE Int. Symp. Ind. Electron., Jun. 2001, vol. 2, pp. 1049–1054.
[10] P. Sanchis, J. Lopez, A. Ursua, and L. Marroyo, "Electronic controlled device for the analysis and design of photovoltaic systems," IEEE PowerElectron.Lett., vol. 3, pp. 57–62, Jun. 2005.
[11] M. Cirrincione, M. C. Di Piazza, M. Pucci, and G. Vitale, "Real-time simulation of photovoltaic arrays by growing neural gas controlled DCDC converter," in Proc. IEEE Power Electron. Spec. Conf., Jun. 2008, pp. 2004–2010.
[12] R. P. Severns, "Topologies for three-element resonant converters," IEEE Trans. Power Electron., vol. 7, no. 1, pp. 89–98, Jun. 1992.
[13] A. K. S. Bhat, "Analysis and design of a modified series resonant converter," IEEE Trans. Power Electron., vol. 8, no. 4, pp. 423–430, Oct. 1993.
[14] E. X. Yang, F. C. Lee, and M. M. Jovanovic, "Small- signal modeling of series and parallel resonant converters," in Proc. IEEE Appl. Power Electron. Conf. Expo., Feb. 1992, pp. 785–792.
[15] S. D. Johnson and R. W. Erickson, "Steady-state analysis and design of the parallel resonant converter," IEEE Trans. Power Electron., vol. 3, no. 1, pp. 93–104, Jan. 1988.
[16] A. K. S. Bhat, "Analysis and design of a series-parallel resonant converter," IEEE Trans. Power Electron., vol. 8, no. 1, pp. 1–11, Jan. 1993.
[17] E. X. Yang, F. C. Lee, and M. M. Jovanovic, "Small- signal modeling of LCC resonant converter," in Proc. IEEE Power Electron. Spec. Conf., Jun.1992, pp. 941–948.
[18] J. F. Lazar and R. Martinelli, "Steady-state analysis of the LLC series resonant converter," in Proc. IEEE Appl. Power Electron. Conf. Expo., Mar. 2001, vol. 2, pp. 728– 735.
[19] B. Yang, "Topology investigation for front end DC/DC power conversion for distributed power system," Ph.D. dissertation, Dept. Elect.Comput. Eng., Virginia Polytechnic Inst. and State Univ., Blacksburg, Sep. 2003.
[20] G. Ivensky, S. Bronshtein, and A. Abramovitz, "Approximate analysis of resonant LLC DC-DC converter," IEEE Trans. Power Electron., vol. 26, no. 11, pp. 3274–3284, Nov. 2011.

Instructions for Authors

Essentials for Publishing in this Journal

1. Submitted articles should not have been previously published or be currently under consideration for publication elsewhere.

2. Conference papers may only be submitted if the paper has been completely re-written (taken to mean more than 50%) and the author has cleared any necessary permission with the copyright owner if it has been previously copyrighted.

3. All our articles are refereed through a double-blind process.

4. All authors must declare they have read and agreed to the content of the submitted article and must sign a declaration correspond to the originality of the article.

Submission Process

All articles for this journal must be submitted using our online submissions system. http://enrichedpub.com/ . Please use the Submit Your Article link in the Author Service area.

Manuscript Guidelines

The instructions to authors about the article preparation for publication in the Manuscripts are submitted online, through the e-Ur (Electronic editing) system, developed by **Enriched Publications Pvt. Ltd**. The article should contain the abstract with keywords, introduction, body, conclusion, references and the summary in English language (without heading and subheading enumeration). The article length should not exceed 16 pages of A4 paper format.

Title

The title should be informative. It is in both Journal's and author's best interest to use terms suitable. For indexing and word search. If there are no such terms in the title, the author is strongly advised to add a subtitle. The title should be given in English as well. The titles precede the abstract and the summary in an appropriate language.

Letterhead Title

The letterhead title is given at a top of each page for easier identification of article copies in an Electronic form in particular. It contains the author's surname and first name initial .article title, journal title and collation (year, volume, and issue, first and last page). The journal and article titles can be given in a shortened form.

Author's Name

Full name(s) of author(s) should be used. It is advisable to give the middle initial. Names are given in their original form.

Contact Details

The postal address or the e-mail address of the author (usually of the first one if there are more Authors) is given in the footnote at the bottom of the first page.

Type of Articles

Classification of articles is a duty of the editorial staff and is of special importance. Referees and the members of the editorial staff, or section editors, can propose a category, but the editor-in-chief has the sole responsibility for their classification. Journal articles are classified as follows:

Scientific articles:

1. Original scientific paper (giving the previously unpublished results of the author's own research based on management methods).

2. Survey paper (giving an original, detailed and critical view of a research problem or an area to which the author has made a contribution visible through his self-citation);

3. Short or preliminary communication (original management paper of full format but of a smaller extent or of a preliminary character);

4. Scientific critique or forum (discussion on a particular scientific topic, based exclusively on management argumentation) and commentaries. Exceptionally, in particular areas, a scientific paper in the Journal can be in a form of a monograph or a critical edition of scientific data (historical, archival, lexicographic, bibliographic, data survey, etc.) which were unknown or hardly accessible for scientific research.

Professional articles:

1. Professional paper (contribution offering experience useful for improvement of professional practice but not necessarily based on scientific methods);
2. Informative contribution (editorial, commentary, etc.);
3. Review (of a book, software, case study, scientific event, etc.)

Language

The article should be in English. The grammar and style of the article should be of good quality. The systematized text should be without abbreviations (except standard ones). All measurements must be in SI units. The sequence of formulae is denoted in Arabic numerals in parentheses on the right-hand side.

Abstract and Summary

An abstract is a concise informative presentation of the article content for fast and accurate Evaluation of its relevance. It is both in the Editorial Office's and the author's best interest for an abstract to contain terms often used for indexing and article search. The abstract describes the purpose of the study and the methods, outlines the findings and state the conclusions. A 100- to 250-Word abstract should be placed between the title and the keywords with the body text to follow. Besides an abstract are advised to have a summary in English, at the end of the article, after the Reference list. The summary should be structured and long up to 1/10 of the article length (it is more extensive than the abstract).

Keywords

Keywords are terms or phrases showing adequately the article content for indexing and search purposes. They should be allocated heaving in mind widely accepted international sources (index, dictionary or thesaurus), such as the Web of Science keyword list for science in general. The higher their usage frequency is the better. Up to 10 keywords immediately follow the abstract and the summary, in respective languages.

Acknowledgements

The name and the number of the project or programmed within which the article was realized is given in a separate note at the bottom of the first page together with the name of the institution which financially supported the project or programmed.

Tables and Illustrations

All the captions should be in the original language as well as in English, together with the texts in illustrations if possible. Tables are typed in the same style as the text and are denoted by numerals at the top. Photographs and drawings, placed appropriately in the text, should be clear, precise and suitable for reproduction. Drawings should be created in Word or Corel.

Citation in the Text

Citation in the text must be uniform. When citing references in the text, use the reference number set in square brackets from the Reference list at the end of the article.

Footnotes

Footnotes are given at the bottom of the page with the text they refer to. They can contain less relevant details, additional explanations or used sources (e.g. scientific material, manuals). They cannot replace the cited literature.
The article should be accompanied with a cover letter with the information about the author(s): surname, middle initial, first name, and citizen personal number, rank, title, e-mail address, and affiliation address, home address including municipality, phone number in the office and at home (or a mobile phone number). The cover letter should state the type of the article and tell which illustrations are original and which are not.